Efficacy of the anti–IL-6 receptor antibody tocilizumab in neuromyelitis optica

A pilot study

OPEN

Manabu Araki, MD, PhD
Takako Matsuoka, MD
Katsuichi Miyamoto, MD, PhD
Susumu Kusunoki, MD, PhD
Tomoko Okamoto, MD, PhD
Miho Murata, MD, PhD
Sachiko Miyake, MD, PhD
Toshimasa Aranami, MD, PhD
Takashi Yamamura, MD, PhD

Correspondence to Dr. Yamamura: yamamura@ncnp.go.jp

ABSTRACT

Objective: To evaluate the safety and efficacy of a humanized anti-interleukin-6 receptor antibody, tocilizumab (TCZ), in patients with neuromyelitis optica (NMO).

Methods: Seven patients with anti-aquaporin-4 antibody (AQP4-Ab)-positive NMO or NMO spectrum disorders were recruited on the basis of their limited responsiveness to their current treatment. They were given a monthly injection of TCZ (8 mg/kg) with their current therapy for a year. We evaluated the annualized relapse rate, the Expanded Disability Status Scale score, and numerical rating scales for neurogenic pain and fatigue. Serum levels of anti-AQP4-Ab were measured with AQP4-transfected cells.

Results: Six females and one male with NMO were enrolled. After a year of TCZ treatment, the annualized relapse rate decreased from 2.9 ± 1.1 to 0.4 ± 0.8 ($p < 0.005$). The Expanded Disability Status Scale score, neuropathic pain, and general fatigue also declined significantly. The ameliorating effects on intractable pain exceeded expectations.

Conclusion: Interleukin-6 receptor blockade is a promising therapeutic option for NMO.

Classification of evidence: This study provides Class IV evidence that in patients with NMO, TCZ reduces relapse rate, neuropathic pain, and fatigue. ***Neurology*® 2014;82:1302–1306**

GLOSSARY

Ab = antibody; **AQP4** = aquaporin-4; **AZA** = azathioprine; **EDSS** = Expanded Disability Status Scale; **IL** = interleukin; **IL-6R** = interleukin-6 receptor; **NMO** = neuromyelitis optica; **PB** = plasmablasts; **PSL** = prednisolone; **TCZ** = tocilizumab.

Neuromyelitis optica (NMO) is a relatively rare autoimmune disease that predominantly affects the spinal cord and optic nerve. Anti–aquaporin-4 antibody (AQP4-Ab), which is a disease marker of NMO, has an important role in causing the destruction of astrocytes that express AQP4.[1] Empirically, the use of disease-modifying drugs for multiple sclerosis, including interferon β, is not recommended for NMO,[2] which is consistent with the distinct pathogenesis of NMO and multiple sclerosis. We have recently described that plasmablasts (PB), which are a subpopulation of B cells, increased in the peripheral blood of patients with NMO and that PB are a major source of anti-AQP4-Ab among peripheral blood B cells.[3] In addition, we observed that exogenous interleukin (IL)-6 promotes the survival of PB and their production of anti-AQP4-Ab in vitro. Given the increased levels of IL-6 in the serum and CSF during relapses of NMO,[1,3] we postulated that blocking IL-6 receptor (IL-6R) pathways might reduce the disease activity of NMO by inactivating the effector functions of PB. A humanized anti–IL-6R monoclonal antibody, tocilizumab (TCZ) (Actemra/RoActemra), has been approved in more than 100 countries for use in the treatment of rheumatoid arthritis.[4] Herein, we describe our clinical study that aimed to explore the efficacy of TCZ in NMO.

Editorial, page 1294

From the Multiple Sclerosis Center (M.A., T.O., S.M., T.A., T.Y.) and Department of Neurology (T.O., M.M.), National Center Hospital, and Department of Immunology, National Institute of Neuroscience (T.M., S.M., T.A., T.Y.), National Center of Neurology and Psychiatry, Tokyo; Department of Neurology (K.M., S.K.), Kinki University School of Medicine, Osaka; and Department of Pediatrics (T.M.), Graduate School of Medicine, University of Tokyo, Japan.

Go to Neurology.org for full disclosures. Funding information and disclosures deemed relevant by the authors, if any, are provided at the end of the article.

Table Demographics of the patients

	Patient						
	1	2	3	4	5	6	7
Age, y/sex	37/F	38/F	26/F	31/M	55/F	62/F	23/F
Age at onset, y	23	27	21	12	38	60	21
Anti-AQP4-Ab	+	+	+	+	+	+	+
Myelitis	+	+	+	+	+	+	–
Optic neuritis	+	+	+	+	+	+	+
EDSS score	3.5	6.5	3.5	6.0	6.5	6.5	3.0
Total no. of relapses	20	9	6	16	20	3	7
ARR before TCZ	3	2	2	2	3	3	5
Immunotherapies for exacerbations	IVMP, PLEX	IVMP, PLEX	IVMP, PLEX	IVMP, OBP, PLEX	IVMP, PLEX	IVMP, PLEX	IVMP, PLEX
Past immunotherapies	IFNβ, IVIg	IFNβ	—	IFNβ, MITX	IFNβ, AZA	—	AZA
Present immunotherapies	PSL, AZA	AZA	PSL	PSL, AZA	PSL, CyA	PSL, CyA	PSL, tacrolimus
Neuropathic pain (e.g., girdle pain), NRS	4	4	2	4	4	3	0
General fatigue, NRS	5	8	6	7	5	3	9
Pain and antispasticity medication	GBP, CZP, NTP, NSAID	CZP, mexiletine, NTP, tizanidine, NSAID	—	CBZ, baclofen, NSAID	CBZ	PGB	—

Abbreviations: AQP4-Ab = aquaporin-4 antibody; ARR = annualized relapse rate; AZA = azathioprine; CBZ = carbamazepine; CZP = clonazepam; CyA = cyclosporine; EDSS = Expanded Disability Status Scale; GBP = gabapentin; IFNβ = interferon β; IVIg = IV immunoglobulin; IVMP = IV methylprednisolone; MITX = mitoxantrone; NRS = numerical rating scale; NSAID = nonsteroidal anti-inflammatory drug; NTP = Neurotropin (an extract from the inflamed skin of vaccinia virus-inoculated rabbits); OBP = oral betamethasone pulse therapy; PGB = pregabalin; PLEX = plasma exchange; PSL = prednisolone; TCZ = tocilizumab.

METHODS **Level of evidence.** The aim of this Class IV evidence study was to evaluate the effect and safety of a monthly injection of TCZ (8 mg/kg) with their current therapy in patients with NMO. We evaluated the adverse events based on Common Terminology Criteria for Adverse Events, version 4.0.

Standard protocol approvals, registrations, and patient consents. All patients gave written informed consent before the first treatment with TCZ. The institutional ethical standards committee on human experimentation approved this clinical study. The study is registered with University Hospital Medical Information Network Clinical Trials Registry, numbers UMIN000005889 and UMIN000007866.

Patients and treatment. Seven patients who met the diagnostic criteria of NMO in 2006 were enrolled after providing informed consent (table). Results of chest x-rays, interferon γ release assays, and plasma 1,3-β-D-glucan measurement excluded latent tuberculosis and fungal infection. All of the patients had been treated with combinations of oral prednisolone (PSL) and immunosuppressants, including azathioprine (AZA). Nevertheless, they had at least 2 relapses during the year before enrollment (figure 1). Among their past immunomodulatory medications, interferon β had been prescribed in 4 patients before the anti-AQP4-Ab assay became available. Although symptomatic treatments had been provided, the patients experienced general fatigue and intractable pain in their trunk and limbs. There were no abnormalities in their routine laboratory blood tests. Neither pleocytosis nor increased levels of IL-6 were observed in the CSF. MRI revealed high-intensity signals in the optic nerves and longitudinally extensive lesions in the spinal cord. All patients except one had scattered brain lesions. A monthly dose (8 mg/kg) of TCZ was added to the patients' oral corticosteroid and immunosuppressive drug regimen.

Clinical and laboratory assessment. As clinical outcome measures, we evaluated alterations in the number of relapses, Expanded Disability Status Scale (EDSS) scores, and pain and fatigue severity scores (numerical rating scales). A relapse was defined as an objective exacerbation in neurologic findings that lasted for longer than 24 hours with an increase in the EDSS score of more than 0.5. Brain and spinal cord MRI scans were examined every 4 or 6 months. CSF examinations, sensory-evoked potentials, and visual-evoked potentials were also evaluated at the time of entry into the study and 12 months later. We measured serum anti-AQP4-Ab levels by evaluating the binding of serum immunoglobulin G to AQP4 transfectants, as previously described.[5] All outcome measures were analyzed with nonparametric Wilcoxon rank-sum tests, with the use of 2-tailed statistical tests at a significance level of 0.05.

RESULTS After starting TCZ treatment, the total number of annual relapses in the patients significantly reduced (figures 1 and 2). Notably, 5 of the 7 patients were relapse-free after starting TCZ. The relapses observed in patients 1 and 5 were mild and their symptoms recovered after IV methylprednisolone. On average, the annualized relapse rate reduced from 2.9 ± 1.1 (range, 2–5) during the year before study to 0.4 ± 0.8 (range, 0–2) during the year after

Figure 1 Clinical course of the patients before and after tocilizumab treatment

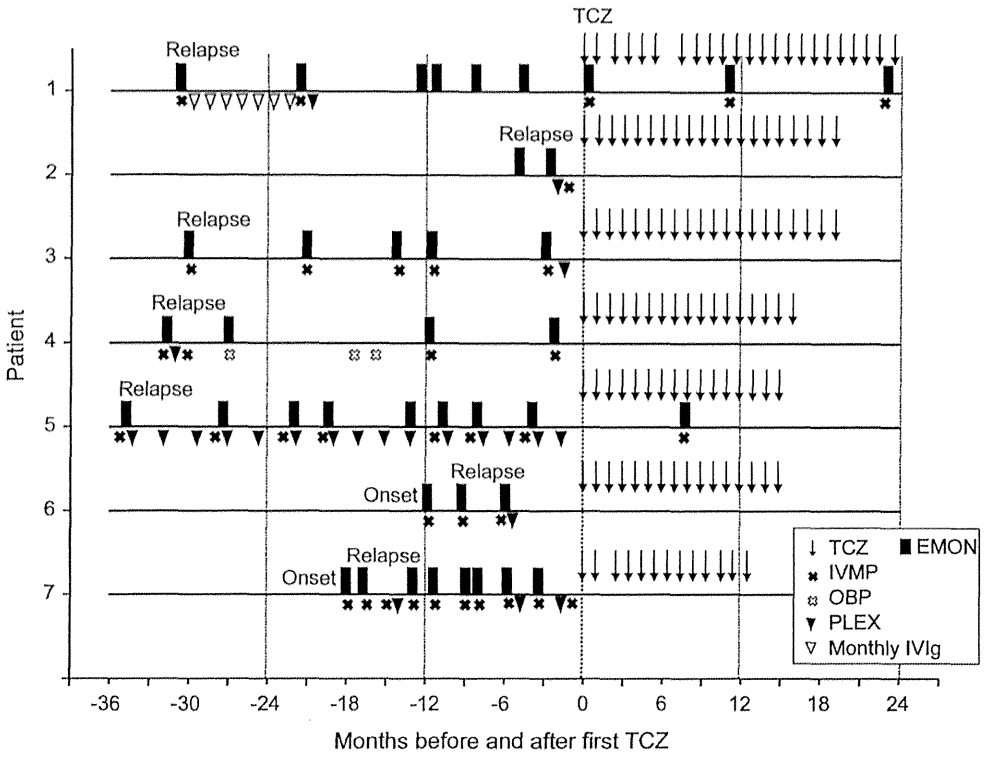

The zero on the x-axis represents the first administration of tocilizumab (TCZ). Dark gray bars: exacerbations of myelitis or optic neuritis (EMON); downward arrow: TCZ treatment; black X: IV methylprednisolone (IVMP); white X: oral betamethasone pulse (OBP) therapy; black triangle: plasma exchange (PLEX); white triangle: IV immunoglobulin (IVIg). After receiving 12 injections, all patients continued treatment with TCZ by entering an extension study that evaluates the long-term safety and efficacy of TCZ. We showed the clinical status after completion of the 1-year study to indicate the continuation of remission.

starting TCZ (figure 2). The EDSS score decreased modestly but significantly from 5.1 ± 1.7 (range, 3.0–6.5) to 4.1 ± 1.6 (range, 2.0–6.0) at 12 months. The chronic neurogenic pain in their trunk and extremities, which is characteristic of NMO[6,7] (table), gradually lessened after the patients started TCZ. Consequently, the numerical rating scale for pain reduced from 3.0 ± 1.5 upon study entry to 1.3 ± 1.3 after 6 months and 0.9 ± 1.2 after 12 months. General fatigue also improved from 6.1 ± 2.0 to 3.9 ± 2.1 at 6 months and 3.0 ± 1.4 at 12 months. The MRI scans, sensory- and visual-evoked potentials, and CSF observations did not show any interval changes. Serum anti-AQP4-Ab levels represented by the relative mean fluorescence intensity were significantly reduced (figure 2E).

Adverse events included upper respiratory infections (patients 1 and 7), acute enterocolitis (patients 1 and 4), acute pyelonephritis (patient 1), leukocytopenia and/or lymphocytopenia (patients 1, 4, and 7), anemia (patients 3 and 7), and a slight decline in systolic blood pressure (patient 1). However, none of the events was severe. Oral PSL and AZA were tapered in patients 1, 3, 4, and 7, resulting in a reduction of the mean doses (PSL from 19.5 ± 7.6 to 8.8 ± 5.6 mg/d [average of patients 1, 3, 4, and 7], AZA from 37.5 to 5.4 mg/d [average of patients 1 and 4]).

DISCUSSION Pain management is a difficult problem in patients with NMO. In fact, a retrospective study of 29 patients with NMO who experienced pain has documented that 22 of the 29 patients were taking pain medications, but none of them rated their current pain as 0 out of 10 on a 10-point scale.[6] In the present study, the intractable pain reduced gradually after the patients started TCZ treatment. After 6 or 12 months of therapy, 3 of the 6 patients with pain were completely free of pain. These results suggested a role of IL-6 in NMO pain and the possible merits of the use of TCZ in clinical practice as a pain reliever.

The pathophysiology of neurogenic pain is now understood in the context of interactions between the immune and nervous systems,[8] which involve proinflammatory cytokines such as IL-6 as well as immune cells, activated glia cells, and neurons. Supportive for the role of IL-6 in pain, recent work in

Figure 2 Effects of tocilizumab on clinical and immunologic parameters

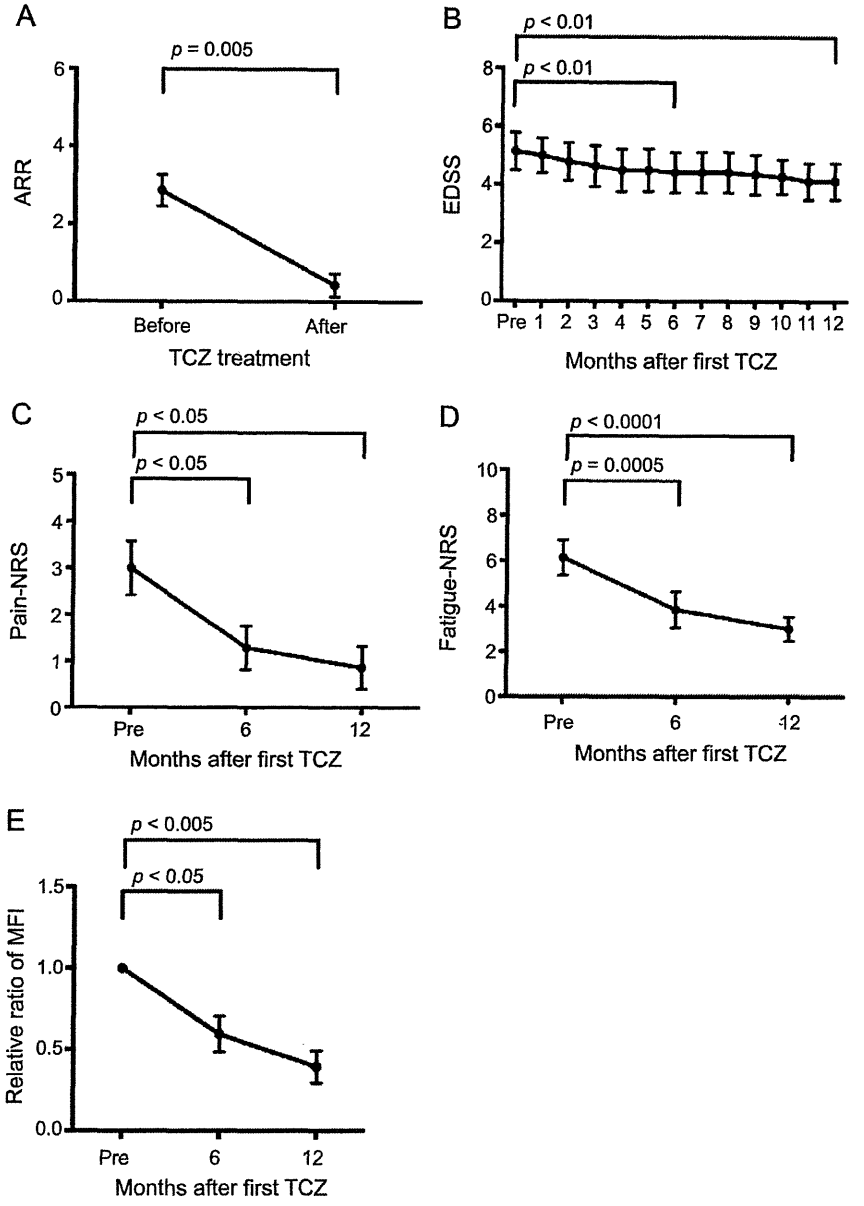

(A) Annualized relapse rate (ARR) before and after tocilizumab (TCZ) treatment. (B) Expanded Disability Status Scale (EDSS) score during the 1-year study period. Pain severity (numerical rating scale [NRS]) (C) and fatigue severity (D) scores before, 6 months after, and 12 months after the start of TCZ treatment. The dots and I bars indicate means ± SEM. We analyzed only data obtained during the first year of TCZ treatment. (E) The alterations in the serum anti-aquaporin-4 antibody (AQP4-Ab) were evaluated by the relative ratio of the mean fluorescence intensity (MFI), which was based on the MFI before TCZ treatment. Serum anti-AQP4-Ab detection assay was performed as described previously[3,5] with minor modifications. In brief, optimally diluted serum was added to human AQP4-expressing Chinese hamster ovary (CHO) cells. CHO cell-bound anti-AQP4-Ab was detected using fluorescein isothiocyanate-anti-human immunoglobulin G antibody by flow cytometry. For comparison, the MFI of each sample was divided by the MFI of the sample before the start of TCZ treatment.

rodents showed that gp130 expressed by nociceptive neurons might have a key role in pathologic pain.[9] Although expression of membrane-bound IL-6R is restricted to hepatocytes, neutrophils, and subsets of T cells, the gp130, ubiquitously expressed in cellular membranes, can transduce IL-6R signaling via binding to the IL-6/soluble IL-6R complex.[4] This indicates that IL-6 trans-signaling via the soluble IL-6R could be pivotal in causing pain in NMO, although alternative possibilities cannot be excluded.

TCZ treatment recently showed efficacy for patients with aggressive NMO who were refractory to the anti-CD20 antibody rituximab.[10] The efficacy of TCZ could result from its effect on IL-6–dependent inflammatory

processes, involving CD20-negative PB, pathogenic T cells, and regulatory T cells. This work, however, does not restrict the use of TCZ in serious NMO. Although the need for monitoring latent infection and adverse events is obvious, we propose that the use of TCZ may be considered at an early stage of NMO before disability or a lower quality of life becomes evident.

AUTHOR CONTRIBUTIONS

T.Y., S.M., S.K., M.M., and M.A.: design and conceptualization of the study. M.A., K.M., T.O., and T.Y.: analysis and internalization of the data. T.M. and T.A.: flow cytometry analysis and anti-AQP4-Ab assay. M.A. and T.Y.: drafting and revising of the manuscript. T.Y.: supervising the entire project.

STUDY FUNDING

Supported by the Health and Labour Sciences Research Grants on Intractable Diseases (Neuroimmunological Diseases) and on Promotion of Drug Development from the Ministry of Health, Labour and Welfare of Japan.

DISCLOSURE

M. Araki has received honoraria from Novartis. T. Matsuoka reports no disclosures relevant to the manuscript. K. Miyamoto has received honoraria from Novartis, Bayer, and Biogen Idec. S. Kusunoki serves as an editorial board member of *Experimental Neurology*, *Journal of Neuroimmunology*, and *Neurology & Clinical Neuroscience* (associate editor). He received honoraria from Teijin Pharma, Nihon Pharmaceuticals, Japan Blood Products Organization, Novartis Pharma, Dainippon Sumitomo Pharma, Kyowa Kirin, Asahi Kasei, Bayer, Sanofi, and GlaxoSmithKline. He is funded by research grants from the Ministry of Health, Labour and Welfare, Japan, and grants from the Japan Science and Technology Agency and the Ministry of Education, Culture, Sports, Science and Technology, Japan. He received research support from Novartis, GlaxoSmithKline, Dainippon Sumitomo Pharma, Teijin Pharma, Astellas, Sanofi, Japan Blood Products Organization, and Nihon Pharmaceuticals. T. Okamoto reports no disclosures relevant to the manuscript. M. Murata received honoraria for consulting and/or lecturing from GlaxoSmithKline Co., Ltd., Boehringer Ingelheim Co., Ltd., Dainippon Sumitomo Pharma Co., Ltd., Novartis Pharma, and Hisamitsu Pharma. S. Miyake has received speaker honoraria from Biogen Idec, Pfizer Inc., and Novartis Pharma. T. Aranami reports no disclosures relevant to the manuscript. T. Yamamura has served on scientific advisory boards for Biogen Idec and Chugai Pharmaceutical Co., Ltd.; has received research support from Ono Pharmaceutical Co., Ltd., Chugai Pharmaceutical Co., Ltd., Teva Pharmaceutical K.K., Mitsubishi Tanabe Pharma Corporation, and Asahi Kasei Kuraray Medical Co., Ltd.; has received speaker honoraria from Novartis Pharma, Nihon Pharmaceutical Co., Ltd., Santen Pharmaceutical Co., Ltd., Abbott Japan Co., Ltd./Eisai Co., Ltd., Biogen Idec, Dainippon Sumitomo Pharma Co., Ltd., Mitsubishi Tanabe Pharma Corporation, Bayer Holding Ltd., and Astellas Pharma Inc. Go to Neurology.org for full disclosures.

Received September 4, 2013. Accepted in final form December 2, 2013.

REFERENCES

1. Jarius S, Wildemann B. AQP4 antibodies in neuromyelitis optica: diagnostic and pathogenetic relevance. Nat Rev Neurol 2010;6:383–392.
2. Okamoto T, Ogawa M, Lin Y, et al. Treatment of neuromyelitis optica: current debate. Ther Adv Neurol Disord 2008;1:5–12.
3. Chihara N, Aranami T, Sato W, et al. Interleukin 6 signaling promotes anti-aquaporin 4 autoantibody production from plasmablasts in neuromyelitis optica. Proc Natl Acad Sci U S A 2011;108:3701–3706.
4. Tanaka T, Narazaki M, Kishimoto T. Therapeutic targeting of the interleukin-6 receptor. Annu Rev Pharmacol Toxicol 2012;52:199–219.
5. Araki M, Aranami T, Matsuoka T, et al. Clinical improvement in a patient with neuromyelitis optica following therapy with the anti-IL-6 receptor monoclonal antibody tocilizumab. Mod Rheumatol 2013;23:827–831.
6. Qian P, Lancia S, Alvarez E, et al. Association of neuromyelitis optica with severe and intractable pain. Arch Neurol 2012;69:1482–1487.
7. Kanamori Y, Nakashima I, Takai Y, et al. Pain in neuromyelitis optica and its effect on quality of life: a cross-sectional study. Neurology 2011;77:652–658.
8. Vallejo R, Tilley DM, Vogel L, et al. The role of glia and immune system in the development and maintenance of neuropathic pain. Pain Pract 2010;10:167–184.
9. Andratsch M, Mair N, Constantin CE, et al. A key role for gp130 expressed on peripheral sensory nerves in pathological pain. J Neurosci 2009;29:13473–13483.
10. Ayzenberg I, Kleiter I, Schröder A, et al. Interleukin 6 receptor blockade in patients with neuromyelitis optica nonresponsive to anti-CD20 therapy. JAMA Neurol 2013;70:394–397.

Biochemical and Biophysical Research Communications 444 (2014) 235–240

Contents lists available at ScienceDirect

Biochemical and Biophysical Research Communications

journal homepage: www.elsevier.com/locate/ybbrc

OX40 ligand regulates splenic CD8$^-$ dendritic cell-induced Th2 responses *in vivo*

Fumitaka Kamachi [a], Norihiro Harada [a,b], Yoshihiko Usui [a,c], Tamami Sakanishi [d], Naoto Ishii [e], Ko Okumura [a], Sachiko Miyake [a], Hisaya Akiba [a,*]

[a] Department of Immunology, Juntendo University, 2-1-1 Hongo, Bunkyo-ku, Tokyo 113-8421, Japan
[b] Department of Respiratory Medicine, Juntendo University, 2-1-1 Hongo, Bunkyo-ku, Tokyo 113-8421, Japan
[c] Department of Ophthalmology, Tokyo Medical University, 6-7-1 Nishi-Shinjuku-ku, Tokyo 160-0023, Japan
[d] Division of Cell Biology, Juntendo University, 2-1-1 Hongo, Bunkyo-ku, Tokyo 113-8421, Japan
[e] Department of Microbiology and Immunology, Tohoku University Graduate School of Medicine, 2-1 Seiryo-machi, Aoba-ku, Sendai, Miyagi 980-8575, Japan

ARTICLE INFO

Article history:
Received 20 December 2013
Available online 22 January 2014

Keywords:
OX40 ligand
Costimulation
Th2 response
Dendritic cell

ABSTRACT

In mice, splenic conventional dendritic cells (cDCs) can be separated, based on their expression of CD8α into CD8$^-$ and CD8$^+$ cDCs. Although previous experiments demonstrated that injection of antigen (Ag)-pulsed CD8$^-$ cDCs into mice induced CD4 T cell differentiation toward Th2 cells, the mechanism involved is unclear. In the current study, we investigated whether OX40 ligand (OX40L) on CD8$^-$ cDCs contributes to the induction of Th2 responses by Ag-pulsed CD8$^-$ cDCs *in vivo*, because OX40–OX40L interactions may play a preferential role in Th2 cell development. When unseparated Ag-pulsed OX40L-deficient cDCs were injected into syngeneic BALB/c mice, Th2 cytokine (IL-4, IL-5, and IL-10) production in lymph node cells was significantly reduced. Splenic cDCs were separated to CD8$^-$ and CD8$^+$ cDCs. OX40L expression was not observed on freshly isolated CD8$^-$ cDCs, but was induced by anti-CD40 mAb stimulation for 24 h. Administration of neutralizing anti-OX40L mAb significantly inhibited IL-4, IL-5, and IL-10 production induced by Ag-pulsed CD8$^-$ cDC injection. Moreover, administration of anti-OX40L mAb with Ag-pulsed CD8$^-$ cDCs during a secondary response also significantly inhibited Th2 cytokine production. Thus, OX40L on CD8$^-$ cDCs physiologically contributes to the development of Th2 cells and secondary Th2 responses induced by Ag-pulsed CD8$^-$ cDCs *in vivo*.

1. Introduction

Dendritic cells (DCs) are professional antigen-presenting cells critical for the induction of adaptive immune responses. Conventional DCs (cDCs) are specialized for antigen processing and presentation to T cells and can be subdivided by their surface expression of CD8α and CD4 as CD8$^-$CD4$^+$, CD8$^-$CD4$^-$, and CD8$^+$CD4$^-$ cDCs in the spleen [1–4]. Both CD8$^-$CD4$^+$ and CD8$^-$CD4$^-$ cDCs appear functionally similar and are referred to as CD8$^-$ cDCs [2,3]. In contrast, the physiologic functions of both CD8$^-$ cDCs and CD8$^+$ cDCs markedly differ. *In vivo* experiments demonstrated that injection of antigen-pulsed CD8$^-$ cDCs induced CD4 T cell differentiation toward Th2 responses (high levels of IL-4, IL-5, and IL-10) whereas antigen-pulsed CD8$^+$ cDCs induced Th1 responses (high levels of IFN-γ [5]. The ability of CD8$^+$ cDCs to induce Th1 differentiation is explained by their ability to produce IL-12 efficiently [6,7]. However, the mechanisms of Th2 responses induced by CD8$^-$ cDCs are not understood.

CD4 T cell differentiation might be regulated by cytokines and various costimulatory molecules expressed on CD4 T cells, and their cognate ligands expressed on DCs such as OX40 (CD134) costimulatory molecule, a member of the TNF receptor superfamily, and its ligand, OX40L (CD252) [8,9]. OX40 is preferentially expressed on activated CD4 T cells and OX40L is mainly expressed on antigen-presenting cells, including activated DCs, B cells, and macrophages. Recent studies emphasized the role of OX40L on DCs for Th2 polarization. In humans, schistosomal egg antigen induced monocyte-derived DCs to express OX40L, which contributed to the induction of Th2 responses [10]. IL-3-treated plasmacytoid DCs expressed OX40L and induced Th2 responses by promoting CD4 T cells to secrete IL-4, IL-5, and IL-13. Blockade of OX40L significantly inhibited this ability of IL-3-treated plasmacytoid DCs [11]. Moreover, OX40L expressed on thymic stromal lymphopoietin (TSLP)-activated DCs induced naïve CD4 T cells to differentiate into TNF-α$^+$ IL-10$^-$ inflammatory Th2 cells [12]. In mice, OX40L expression on bone marrow-derived DCs (BMDCs) is upregulated downstream of CD40 signaling and is critical for optimal Th2 priming *in vivo* [13]. In contrast to these studies, the use of agonistic anti-OX40 mAb revealed OX40-mediated costimulation enhanced the

* Corresponding author. Fax: +81 3 3813 0421.
E-mail address: hisaya@juntendo.ac.jp (H. Akiba).

0006-291X/$ - see front matter © 2014 Elsevier Inc. All rights reserved.
http://dx.doi.org/10.1016/j.bbrc.2014.01.060

development of Th1 responses induced by splenic CD8$^-$ cDCs *in vivo* [14]. Thus, the function of OX40L on splenic CD8$^-$ cDCs is still controversial. In this study, we examined the physiological contribution of OX40–OX40L interactions on CD8$^-$ cDCs-induced Th2 responses by using blocking anti-OX40L mAb.

2. Materials and methods

2.1. Animals

Female BALB/c mice were purchased from Charles River Laboratories (Kanagawa, Japan). OX40L-deficient mice were generated as previously described [15] and backcrossed for seven generations with BALB/c mice purchased from Oriental Yeast Co. (Tokyo, Japan). All mice were 6–8 week old at the start of experiments and kept under specific pathogen-free conditions during the experiments. All animal experiments were approved by Juntendo University Animal Experimental Ethics Committee.

2.2. Antibodies and reagents

An anti-mouse OX40L (RM134L) mAb was previously generated in our laboratory [16]. Control rat IgG was purchased from Sigma–Aldrich (St Louis, MO, USA). Purified anti-CD40 (HM40-3), allophycocyanin (APC)-conjugated anti-CD8α (53-6.7), and rat IgG isotype control were purchased from eBioscience (San Diego, CA, USA). Purified anti-CD16/32 (2.4G2) and FITC-conjugated anti-CD11c (HL3), recombinant mouse GM-CSF, IL-4, and IFN-γ were purchased from BD Biosciences (San Jose, CA, USA).

2.3. Preparation and stimulation of splenic DCs

To isolate splenic DCs, spleens from BALB/c or OX40L-deficient mice were digested with 400 U/ml of collagenase (Wako Biochemicals, Tokyo, Japan), further dissociated in Ca^{2+}-free medium in the presence of 5 mM EDTA, and separated into low- and high-density fractions by Optiprep-gradient (Axis-Shield, Oslo, Norway) as described previously [17]. Low-density cells were pulsed overnight with 50 μg/ml of keyhole limpet hemocyanin (KLH) in culture medium supplemented with 20 ng/ml of GM-CSF as described previously [5]. After overnight culture, splenic CD11c$^+$ DCs were isolated by incubation with anti-CD11c-coupled magnetic beads and positive selection by autoMACS column (Miltenyi Biotec, Bergisch Gladbach, Germany). CD11c$^+$ DCs were further separated according to CD8α expression by FACS sorting. CD11c$^+$ cells were incubated with FITC-conjugated anti-CD11c and APC-conjugated anti-CD8α mAbs, and two populations (CD8$^+$CD11c$^+$ DCs and CD8$^-$CD11c$^+$ DCs) were sorted by FACSVantage (BD Biosciences). To examine OX40L expression, separated DC populations were incubated with anti-CD40 mAb (10 μg/ml) with IL-4 (20 ng/ml) or IFN-γ (20 ng/ml) in the presence or absence of GM-CSF (20 ng/ml) at 37 °C for 24 h.

2.4. Flow cytometric analysis

Cells were pre-incubated with unlabeled anti-CD16/32 mAb to avoid non-specific binding of Abs to FcγR, incubated with FITC- or APC-labeled mAbs, or biotinylated mAb followed by PE-labeled streptavidin. Stained cells (live cells gated by forward and side scatter profiles and propidium iodide exclusion) were analyzed by FACSCalibur (BD Biosciences), and data were processed by CellQuest (BD Biosciences).

2.5. Immunization protocol

KLH-pulsed splenic cDCs were washed in PBS and immunized (3×10^5 cells) into the hind footpad of BALB/c mice. Some groups of mice ($n = 5$–6) were administered 400 μg of anti-OX40L mAb or rat IgG intraperitoneally (i.p.) at days 0, 1, and 3, or daily from days 0 to 3 and days 14–17. Popliteal lymph node (LN) cells were harvested 5 days after primary or secondary immunizations.

2.6. T cell stimulation in vitro

LN cells were isolated and cultured in RPMI1640 medium (containing 10% FCS, 10 mM HEPES, 2 mM L-glutamine, 0.1 mg/ml penicillin and streptomycin, and 50 μM 2-mercaptoethanol) at a density of 6×10^5 cells/well in the presence of indicated doses of KLH. To assess proliferative responses, cultures were pulsed with tritiated thymidine ([^{3}H]TdR; 0.5 μCi/well; PerkinElmer, Winter Street Waltham, MA, USA) for the last 6 h of a 48 h or 72 h culture and harvested on a Micro 96 Harvester (Molecular Devices, Sunnyvale, CA, USA). Incorporated radioactivity was measured using a microplate beta counter (Micro β Plus; PerkinElmer). To determine cytokine production, cell-free supernatants were collected at 48 h or 72 h and assayed for IL-2, IL-4, IL5, IL-10, and IFN-γ by ELISA using Ready-SET-Go! kits (eBioscience) according to the manufacturer's instructions.

2.7. Statistical analysis

Statistical analyses were performed by unpaired Student *t*-test or Tukey's multiple comparison test. Results are expressed as mean ± SEM. Values of $P < 0.05$ were considered significant.

3. Results

3.1. OX40L is required for optimal Th2 responses induced by splenic cDCs in vivo

Because a previous report demonstrated KLH-pulsed CD8$^-$ and CD8$^+$ cDCs differentially regulated Th cell development, we followed the same protocol using KLH as an antigen. To clarify the contribution of splenic cDC OX40L on CD4 T cell differentiation, we examined CD4 T cell responses induced by splenic OX40L$^{-/-}$ cDCs. cDCs were purified from spleens of OX40L-deficient or wild-type BALB/c mice without treatment, pulsed with KLH during overnight culture with GM-CSF, to isolate CD11c^{high} B220$^-$ cells (cDC population). OX40L$^{-/-}$ cDCs or WT cDCs (3×10^5) were injected into hind footpads of syngeneic BALB/c mice. LNs were prepared on day 5 and proliferative responses and cytokine production against various doses of KLH were assessed. KLH-specific proliferative responses and IL-2 production were reduced in LN cells from OX40L$^{-/-}$ cDCs-injected mice compared with WT cDCs-injected mice (Fig. 1). Th2 cytokine production (IL-4, IL-5, and IL-10) was also significantly reduced in OX40L$^{-/-}$ cDCs-injected mice compared with WT cDCs-injected mice. In contrast, Th1 type cytokine IFN-γ production was non-significantly increased in OX40L$^{-/-}$ cDCs-injected mice compared with WT cDCs-injected mice.

Similar results were obtained when KLH-pulsed OX40L$^{-/-}$ bone marrow-derived DCs (BMDCs) were injected into hind footpads of BALB/c mice (Supplemental Fig. S1). KLH-specific proliferative responses and IL-2 production were reduced in LN cells from OX40L$^{-/-}$ BMDCs-injected mice compared with WT BMDCs-injected mice. Th2 cytokine production (IL-4, IL-5, and IL-10) was significantly reduced in OX40L$^{-/-}$ BMDCs-injected mice, whereas IFN-γ production was similar between OX40L$^{-/-}$ BMDCs-injected

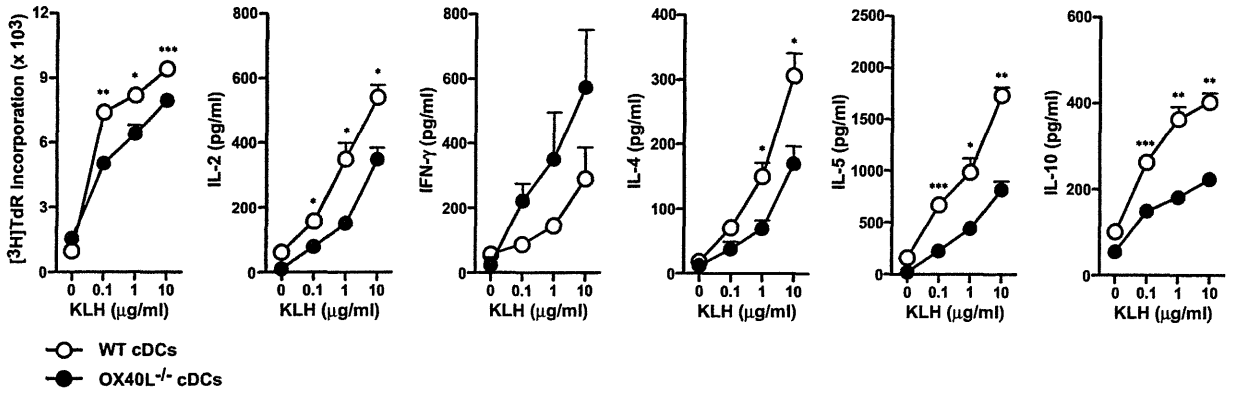

Fig. 1. OX40L is required for optimal Th2 responses by splenic cDCs *in vivo*. BALB/c mouse hind footpads were injected with KLH-pulsed cDCs isolated from the spleen of wild-type BALB/c or OX40L$^{-/-}$ BALB/c mice. LN cells were harvested at day 5 and cultured with indicated doses of KLH. To estimate proliferation, 0.5 μCi ^{3}H-thymidine ([^{3}H]TdR) was added during the last 6 h of a 48 h culture. Production of IFN-γ, IL-2, IL-4, IL-5, and IL-10 in culture supernatants at 48 h was determined by ELISA. Results are presented as mean ± SEM. *$p < 0.05$, **$p < 0.01$, and ***$p < 0.001$. Similar results were obtained in three independent experiments.

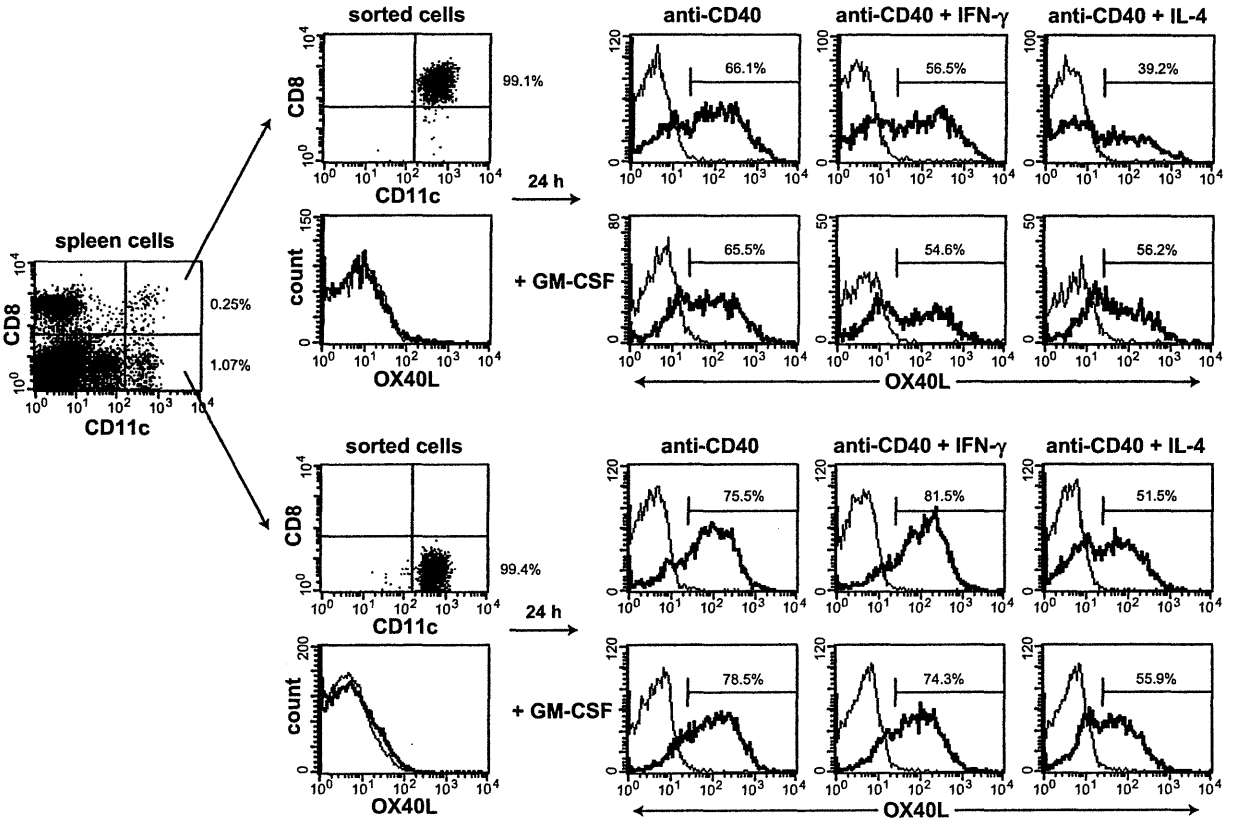

Fig. 2. Expression of OX40L on activated CD8^{-} and CD8^{+} cDCs. Spleen cells were isolated from BALB/c mice and stained with FITC-labeled anti-CD11c, APC-labeled anti-CD8α, and biotinylated anti-OX40L or control IgG followed by PE-labeled streptavidin. CD8^{-}CD11c^{high} and CD8^{+}CD11c^{high} cDCs were isolated from spleens by FACS sorting. Isolated CD8^{-}CD11c^{high} and CD8^{+}CD11c^{high} cDCs were stimulated with anti-CD40 mAb in the presence or absence of GM-CSF, IFN-γ, and IL-4. Cells were harvested at 24 h and stained with anti-OX40L mAb or control rat IgG. Thick lines indicate staining with anti-OX40L mAb and thin lines indicate background staining with control IgG. Data are representative of three experiments.

and WT BMDCs-injected mice. In addition, administration of neutralizing anti-OX40L mAb to WT BMDCs-injected mice significantly reduced Th2 cytokine production similar to OX40L$^{-/-}$ BMDCs-injected mice. Th2 cytokine reduction was also observed in KLH-pulsed WT BMDCs injected with anti-OX40L mAb into IFN-γ-deficient mice (Supplemental Fig. S2). These results indicated a critical role of OX40L in splenic cDCs- and BMDCs-induced Th2 responses *in vivo*. The inhibition of Th2 responses by anti-OX40L treatment was not necessarily a result of a shift to Th1 responses.

3.2. Expression of OX40L on splenic cDCs

The expression of OX40L on two major subsets of splenic cDCs was assessed by flow cytometry. Splenic cDCs were separated

based on CD8α and CD11c expression, into $CD8^-CD11c^{high}$ cDCs ($CD8^-$ cDCs) and $CD8^+CD11c^{high}$ cDCs ($CD8^+$ cDCs), and stimulated with agonistic anti-CD40 with or without cytokines (GM-CSF, IFN-γ, or IL-4) for 24 h (Fig. 2). While OX40L expression was not observed on freshly isolated $CD8^-$ or $CD8^+$ cDCs, it was induced by anti-CD40 mAb stimulation. Addition of IL-4 reduced OX40L expression on anti-CD40-stimulated $CD8^-$ and $CD8^+$ cDCs, whereas OX40L expression was not affected by the addition of GM-CSF or IFN-γ.

3.3. *Effect of anti-OX40L mAb on the development of Th2 responses induced by KLH-pulsed $CD8^-$ cDCs in vivo*

We next examined whether KLH-pulsed $CD8^-$ cDCs could induce Th2 responses compared with KLH-pulsed $CD8^+$ cDCs, and whether OX40L contributes to $CD8^-$ cDCs-induced Th2 responses. BALB/c mice were injected into the hind footpads with KLH-pulsed $CD8^-$ or $CD8^+$ cDCs, and treated with anti-OX40L mAb or control IgG at days 0, 1, and 3. LN cells were isolated at day 5 and KLH-specific proliferative responses and cytokine production were assessed. Consistent with previous reports, IL-4 production by LN cells from $CD8^-$ cDCs-injected mice was significantly higher than in $CD8^+$ cDCs-injected mice (Fig. 3). In contrast, IFN-γ production in $CD8^+$ cDCs-injected mice was non-significantly increased compared with the $CD8^-$ cDCs-injected mice. Proliferative responses and other Th2 cytokine production (IL-5 and IL-10) were similar between $CD8^-$ cDCs-injected and $CD8^+$ cDCs-injected mice. Anti-OX40L mAb administration strongly inhibited IL-4, IL-5, and IL-10 production induced by $CD8^-$ cDCs injection, while IFN-γ was slightly increased. Thus, OX40L has an important role in the development of Th2 responses induced by KLH-pulsed $CD8^-$ cDCs *in vivo*. Furthermore, administration of anti-OX40L mAb reduced IL-4 production induced by $CD8^+$ cDCs injection. Therefore, OX40L may also regulate IL-4 production induced by KLH-pulsed $CD8^+$ cDCs.

3.4. *Effect of anti-OX40L mAb in secondary Th2 responses induced by KLH-pulsed $CD8^-$ cDCs in vivo*

The OX40–OX40L pathway is crucial for recall responses when memory T cells are reactivated [18]. Therefore, we further examined the role of OX40L in secondary Th2 responses induced by KLH-pulsed $CD8^-$ cDCs *in vivo*. BALB/c mice were immunized first into the hind footpads with KLH-pulsed $CD8^-$ cDCs at day 0 and then under the same conditions with KLH-pulsed $CD8^-$ cDCs at day 14. Some groups of mice were treated with anti-OX40L mAb or control IgG daily from days 0 to 3 in the primary phase and days 14–17 in the secondary phase. LN cells were isolated at day 19 and the KLH-specific Th2 cytokine production was assessed. Anti-OX40L mAb administration during the primary phase only, reduced IL-4 and IL-5 production compared with control IgG (Fig. 4). In addition, anti-OX40L mAb administration in the secondary phase strongly inhibited IL-4, IL-5, and IL-10 production compared with control IgG. The inhibitory effect of anti-OX40 mAb

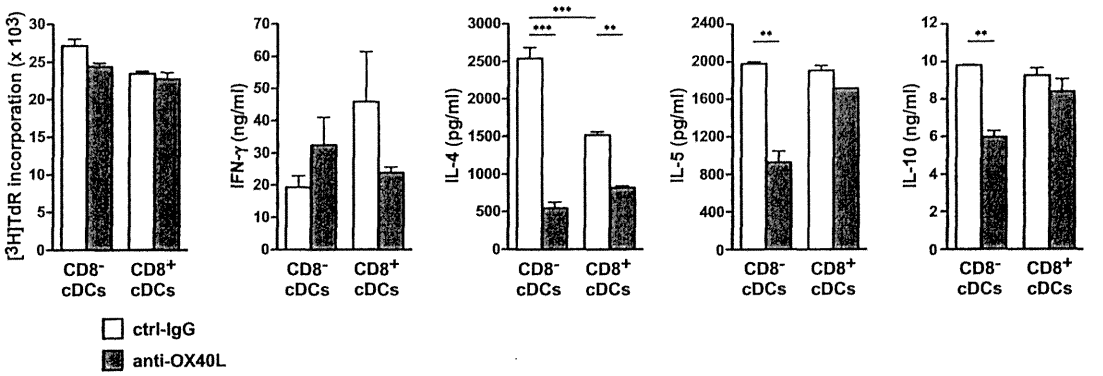

Fig. 3. Effect of anti-OX40L mAb on the development of Th2 responses induced by KLH-pulsed $CD8^-$ cDCs *in vivo*. BALB/c mouse hind footpads were injected with KLH-pulsed $CD8^-$ or $CD8^+$ cDCs. Mice were administered 400 μg of anti-OX40L mAb or control rat IgG (ctrl-IgG) i.p. at days 0, 1, and 3. LN cells were harvested at day 5 and cultured with 20 μg/ml of KLH. To estimate proliferation, 0.5 μCi [^{3}H]TdR was added during the last 6 h of a 72 h culture. Production of IFN-γ, IL-4, IL-5, and IL-10 in the culture supernatants at 72 h was determined by ELISA. Results are presented as mean ± SEM. $^*p < 0.05$, $^{**}p < 0.01$, and $^{***}p < 0.001$. Similar results were obtained in three independent experiments.

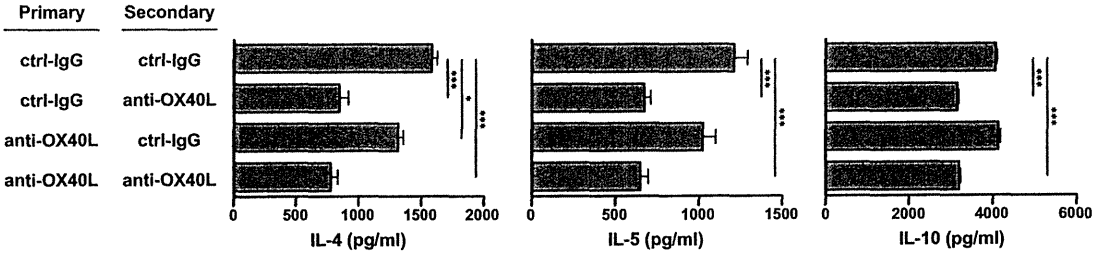

Fig. 4. Effect of anti-OX40L mAb on the development of memory Th2 responses induced by $CD8^-$ cDCs *in vivo*. BALB/c mice were immunized first with KLH-pulsed $CD8^-$ cDCs at day 0 and boosted with the same KLH-pulsed $CD8^-$ cDCs at day 14. Mice were administered 400 μg of anti-OX40L mAb or ctrl-IgG i.p. daily from days 0 to 3 and days 14–17. LN cells were harvested at day 19 and cultured with 10 μg/ml of KLH. To estimate proliferation, 0.5 μCi [^{3}H]TdR was added during the last 6 h of a 72 h culture. Production of IFN-γ, IL-4, IL-5, and IL-10 in culture supernatants at 72 h was determined by ELISA. Results are presented as mean ± SEM. $^*p < 0.05$, $^{**}p < 0.01$, and $^{***}p < 0.001$. Similar results were obtained in three independent experiments.

treatment in the secondary phase was comparable to mice treated with anti-OX40 mAb in both primary and secondary phases. Thus, OX40L might have an important role in both primary and secondary Th2 responses induced by KLH-pulsed $CD8^-$ cDCs *in vivo*.

4. Discussion

The current study investigated the physiological role of splenic $CD8^-$ cDC OX40L to regulate CD4 T cell Th2 differentiation *in vivo*. When antigen KLH-pulsed OX40L-deficient cDCs were injected into BALB/c mice, LN Th2 cytokine production (IL-4, IL-5, and IL-10) was significantly reduced. Splenic cDCs were separated into $CD8^-$ and $CD8^+$ cDCs. A previous study demonstrated that although injection of KLH-pulsed $CD8^-$ cDCs induced CD4 T cell differentiation toward Th2 responses, KLH-pulsed $CD8^+$ cDCs promoted Th1 responses [5]. Consistently, our results indicated that $CD8^-$ cDCs markedly induced IL-4 production and $CD8^+$ cDCs tended to induce IFN-γ production. Administration of neutralizing anti-OX40L mAb significantly inhibited IL-4, IL-5, and IL-10 production induced by KLH-pulsed $CD8^-$ cDCs. Moreover, treatment of anti-OX40L mAb with KLH-pulsed $CD8^-$ cDCs during a secondary response also significantly inhibited Th2 cytokine production. Thus, OX40L contributes to both the development of Th2 cells and secondary Th2 responses induced by KLH-pulsed $CD8^-$ cDCs *in vivo*. However, these findings are inconsistent with a previous report where administration of anti-OX40 mAb enhanced the development of Th1 cells secreting high levels of IFN-γ, but no IL-4 and IL-5, induced by KLH-pulsed $CD8^-$ cDCs *in vivo* [14]. The reason for this discrepancy is not clear, but it may be attributable to differences in experimental conditions. The previous study isolated splenic cDCs from mice treated with FMS-like tyrosine kinase 3 ligand (Flt3L) on 11 days, whereas mice were untreated in our study. Flt3 is a crucial factor in humans and mice to promote the development of cDCs *in vivo* and *in vitro*. However, a bias toward the generation of $CD8^+$ cDCs in the spleen was observed in mice treated with Flt3L [19,20]. The previous study also examined the effect of exogenous OX40 costimulation using agonistic anti-OX40 mAb, suggesting such an effect is not mediated by endogenous OX40–OX40L interactions between CD4 T cells and cDCs. Our results suggest that physiological OX40–OX40L interactions participate in CD4 T cell-$CD8^-$ cDCs interactions, and that OX40L on $CD8^-$ cDCs might contribute to the induction of Th2 responses *in vivo*.

In humans, TSLP-activated DCs can promote the differentiation of naïve CD4 T cells into a Th2 phenotype and the expansion of CD4 Th2 memory cells in an unique manner dependent on OX40L in the absence of IL-12 [12]. TSLP, an IL-7-like cytokine, is produced mainly by damaged epithelial cells and is a key molecule that links epithelial cells and DCs at the interface of allergic inflammation by participating in the programming of DC-mediated Th2 polarization [21–24]. TSLP activates STAT1, STAT3, STAT4, STAT5, and STAT6, whereas the contributions of individual STAT proteins to the activation of DCs is unclear [25]. Most recently, a mouse study demonstrated that DC-specific deletion of STAT5 was critical for TSLP-mediated Th2 differentiation, but not Th1 differentiation [26]. Loss of STAT5 in DCs affected upregulation of OX40L expression in response to TSLP. However, DC subsets in $Stat5^{-/-}$ chimeric mouse spleens had a higher proportion of $CD8^+$ cDCs and a reduced frequency of $CD4^+$ $CD8^-$ cDCs compared with $Stat5^{+/+}$ chimeras, suggesting STAT5 signaling regulates a balanced production of these splenic DC subsets *in vivo* [27]. Thus, STAT5 may be required for OX40L-dependent Th2 cell differentiation induced by KLH-pulsed $CD8^-$ cDCs. To confirm this, further studies are required using STAT5-specific deleted $CD8^-$ cDCs. In this study, we demonstrated that KLH-pulsed $OX40L^{-/-}$ BMDCs injected into hind footpads of BALB/c mice significantly reduced Th2 cytokine production (IL-4, IL-5, and IL-10) in LN cells compared with WT BMDCs-injected mice. Consistent with these observations, it was reported that OX40L expression by GM-CSF-induced BMDCs is required for optimal induction of primary and memory Th2 responses *in vivo* [13]. GM-CSF can activate STAT5, and GM-CSF-activated STAT5 inhibits the transcription of *Irf8* [27], which encodes interferon regulatory factor 8 (IRF8). IRF8 is required for IL-12 production [25], an essential cytokine required for the induction of Th1 responses [28]. Therefore, OX40L-dependent Th2 responses induced by KLH-pulsed $CD8^-$ cDCs might depend on the absence of IL-12, as IL-12 has a dominant effect over OX40L in Th cell differentiation [12]. Indeed, we observed that $CD8^+$ cDCs produced high amounts of IL-12p40 after stimulation with agonistic anti-CD40 mAb, whereas IL12p40 production on $CD8^-$ cDCs was markedly lower (unpublished observation). Taken together, these findings suggest that the development of Th2 responses by KLH-pulsed $CD8^-$ cDCs requires two conditions: the expression of OX40L and the absence of IL-12.

However, whether OX40 signaling on CD4 T cells directly induces Th2 differentiation is still unclear. It is well known that OX40 can bind to TNF receptor-associated factor (TRAF) 2, TRAF3, and TRAF5. However, these molecules also can bind to other TNF receptor family molecules. On a transcriptional basis, it was determined that OX40L expressed by TSLP-DCs induced the expression of GATA-3 in CD4 T cells, supporting their critical role in Th2 polarization [12]. Another study indicated that OX40 enhanced TCR-induced calcium influx, leading to the enhanced nuclear accumulation of NFATc1 and NFATc2, that likely regulates the production of cytokines [29]. More studies are required to determine how OX40 signaling promotes Th2 differentiation.

Acknowledgments

This study was supported by Grants #23390260 and #25461503 from the Ministry of Education, Culture, Sports, Science and Technology, Japan.

The authors thank Dr. J.L. Croxford for critical reading of the paper.

Appendix A. Supplementary data

Supplementary data associated with this article can be found, in the online version, at http://dx.doi.org/10.1016/j.bbrc.2014.01.060.

References

[1] G.T. Belz, S.L. Nutt, Transcriptional programming of the dendritic cell network, Nat. Rev. Immunol. 12 (2012) 101–113.
[2] P. Sathe, K. Shortman, The steady-state development of splenic dendritic cells, Mucosal. Immunol. 1 (2008) 425–431.
[3] R. Kushwah, J. Hu, Complexity of dendritic cell subsets and their function in the host immune system, Immunology 133 (2011) 409–419.
[4] S.S. Watowich, Y.J. Liu, Mechanisms regulating dendritic cell specification and development, Immunol. Rev. 238 (2010) 76–92.
[5] R. Maldonado-Lopez, T. De Smedt, P. Michel, J. Godfroid, B. Pajak, C. Heirman, K. Thielemans, O. Leo, J. Urbain, M. Moser, $CD8a^+$ and $CD8a^-$ subclasses of dendritic cells direct the development of distinct T helper cells in vivo, J. Exp. Med. 189 (1999) 587–592.
[6] H. Hochrein, K. Shortman, D. Vremec, B. Scott, P. Hertzog, M. O'Keeffe, Differential production of IL-12, IFN-a, and IFN-g by mouse dendritic cell subsets, J. Immunol. 166 (2001) 5448–5455.
[7] O. Schulz, A.D. Edwards, M. Schito, J. Aliberti, S. Manickasingham, A. Sher, C. Reis e Sousa, CD40 triggering of heterodimeric IL-12 p70 production by dendritic cells in vivo requires a microbial priming signal, Immunity 13 (2000) 453–462.
[8] M. Croft, Control of immunity by the TNFR-related molecule OX40 (CD134), Annu. Rev. Immunol. 28 (2010) 57–78.
[9] E.C. de Jong, H.H. Smits, M.L. Kapsenberg, Dendritic cell-mediated T cell polarization, Springer Semin. Immunopathol. 26 (2005) 289–307.

[10] E.C. de Jong, P.L. Vieira, P. Kalinski, J.H. Schuitemaker, Y. Tanaka, E.A. Wierenga, M. Yazdanbakhsh, M.L. Kapsenberg, Microbial compounds selectively induce Th1 cell-promoting or Th2 cell-promoting dendritic cells in vitro with diverse th cell-polarizing signals, J. Immunol. 168 (2002) 1704–1709.
[11] T. Ito, R. Amakawa, M. Inaba, T. Hori, M. Ota, K. Nakamura, M. Takebayashi, M. Miyaji, T. Yoshimura, K. Inaba, S. Fukuhara, Plasmacytoid dendritic cells regulate Th cell responses through OX40 ligand and type I IFNs, J. Immunol. 172 (2004) 4253–4259.
[12] T. Ito, Y.H. Wang, O. Duramad, T. Hori, G.J. Delespesse, N. Watanabe, F.X. Qin, Z. Yao, W. Cao, Y.J. Liu, TSLP-activated dendritic cells induce an inflammatory T helper type 2 cell response through OX40 ligand, J. Exp. Med. 202 (2005) 1213–1223.
[13] S.J. Jenkins, G. Perona-Wright, A.G. Worsley, N. Ishii, A.S. MacDonald, Dendritic cell expression of OX40 ligand acts as a costimulatory, not polarizing, signal for optimal Th2 priming and memory induction in vivo, J. Immunol. 179 (2007) 3515–3523.
[14] T. De Smedt, J. Smith, P. Baum, W. Fanslow, E. Butz, C. Maliszewski, Ox40 costimulation enhances the development of T cell responses induced by dendritic cells in vivo, J. Immunol. 168 (2002) 661–670.
[15] K. Murata, N. Ishii, H. Takano, S. Miura, L.C. Ndhlovu, M. Nose, T. Noda, K. Sugamura, Impairment of antigen-presenting cell function in mice lacking expression of OX40 ligand, J. Exp. Med. 191 (2000) 365–374.
[16] H. Akiba, H. Oshima, K. Takeda, M. Atsuta, H. Nakano, A. Nakajima, C. Nohara, H. Yagita, K. Okumura, CD28-independent costimulation of T cells by OX40 ligand and CD70 on activated B cells, J. Immunol. 162 (1999) 7058–7066.
[17] C. Ruedl, C. Rieser, G. Bock, G. Wick, H. Wolf, Phenotypic and functional characterization of CD11c$^+$ dendritic cell population in mouse Peyer's patches, Eur. J. Immunol. 26 (1996) 1801–1806.
[18] S. Salek-Ardakani, J. Song, B.S. Halteman, A.G. Jember, H. Akiba, H. Yagita, M. Croft, OX40 (CD134) controls memory T helper 2 cells that drive lung inflammation, J. Exp. Med. 198 (2003) 315–324.
[19] M. O'Keeffe, H. Hochrein, D. Vremec, J. Pooley, R. Evans, S. Woulfe, K. Shortman, Effects of administration of progenipoietin 1, Flt-3 ligand, granulocyte colony-stimulating factor, and pegylated granulocyte-macrophage colony-stimulating factor on dendritic cell subsets in mice, Blood 99 (2002) 2122–2130.
[20] P. Bjorck, Isolation and characterization of plasmacytoid dendritic cells from Flt3 ligand and granulocyte-macrophage colony-stimulating factor-treated mice, Blood 98 (2001) 3520–3526.
[21] S.L. Friend, S. Hosier, A. Nelson, D. Foxworthe, D.E. Williams, A. Farr, A thymic stromal cell line supports in vitro development of surface IgM$^+$ B cells and produces a novel growth factor affecting B and T lineage cells, Exp. Hematol. 22 (1994) 321–328.
[22] J.E. Sims, D.E. Williams, P.J. Morrissey, K. Garka, D. Foxworthe, V. Price, S.L. Friend, A. Farr, M.A. Bedell, N.A. Jenkins, N.G. Copeland, K. Grabstein, R.J. Paxton, Molecular cloning and biological characterization of a novel murine lymphoid growth factor, J. Exp. Med. 192 (2000) 671–680.
[23] V. Soumelis, P.A. Reche, H. Kanzler, W. Yuan, G. Edward, B. Homey, M. Gilliet, S. Ho, S. Antonenko, A. Lauerma, K. Smith, D. Gorman, S. Zurawski, J. Abrams, S. Menon, T. McClanahan, R. de Waal-Malefyt Rd, F. Bazan, R.A. Kastelein, Y.J. Liu, Human epithelial cells trigger dendritic cell mediated allergic inflammation by producing TSLP, Nat. Immunol. 3 (2002) 673–680.
[24] Y.J. Liu, V. Soumelis, N. Watanabe, T. Ito, Y.H. Wang, W. Malefyt Rde, M. Omori, B. Zhou, S.F. Ziegler, TSLP: an epithelial cell cytokine that regulates T cell differentiation by conditioning dendritic cell maturation, Annu. Rev. Immunol. 25 (2007) 193–219.
[25] K. Arima, N. Watanabe, S. Hanabuchi, M. Chang, S.C. Sun, Y.J. Liu, Distinct signal codes generate dendritic cell functional plasticity, Sci. Signaling 3 (2010) ra4.
[26] B.D. Bell, M. Kitajima, R.P. Larson, T.A. Stoklasek, K. Dang, K. Sakamoto, K.U. Wagner, B. Reizis, L. Hennighausen, S.F. Ziegler, The transcription factor STAT5 is critical in dendritic cells for the development of TH2 but not TH1 responses, Nat. Immunol. 14 (2013) 364–371.
[27] E. Esashi, Y.H. Wang, O. Perng, X.F. Qin, Y.J. Liu, S.S. Watowich, The signal transducer STAT5 inhibits plasmacytoid dendritic cell development by suppressing transcription factor IRF8, Immunity 28 (2008) 509–520.
[28] S.E. Macatonia, N.A. Hosken, M. Litton, P. Vieira, C.S. Hsieh, J.A. Culpepper, M. Wysocka, G. Trinchieri, K.M. Murphy, A. O'Garra, Dendritic cells produce IL-12 and direct the development of Th1 cells from naive CD4$^+$ T cells, J. Immunol. 154 (1995) 5071–5079.
[29] T. So, J. Song, K. Sugie, A. Altman, M. Croft, Signals from OX40 regulate nuclear factor of activated T cells c1 and T cell helper 2 lineage commitment, Proc. Natl. Acad. Sci. U.S.A. 103 (2006) 3740–3745.

ARTHRITIS & RHEUMATOLOGY
Vol. 67, No. 2, February 2015, pp 396–407
DOI 10.1002/art.38924

Ras Guanine Nucleotide–Releasing Protein 4 Is Aberrantly Expressed in the Fibroblast-like Synoviocytes of Patients With Rheumatoid Arthritis and Controls Their Proliferation

Michihito Kono,[1] Shinsuke Yasuda,[1] Richard L. Stevens,[2] Hideyuki Koide,[1] Takashi Kurita,[1] Yuka Shimizu,[1] Yusaku Kanetsuka,[1] Kenji Oku,[1] Toshiyuki Bohgaki,[1] Olga Amengual,[1] Tetsuya Horita,[1] Tomohiro Shimizu,[1] Tokifumi Majima,[1] Takao Koike,[1] and Tatsuya Atsumi[1]

Objective. **Ras guanine nucleotide–releasing protein 4 (RasGRP-4) is a calcium-regulated guanine nucleotide exchange factor and diacylglycerol/phorbol ester receptor not normally expressed in fibroblasts. While RasGRP-4–null mice are resistant to arthritis induced by anti–glucose-6-phosphate isomerase autoantibodies, the relevance of these findings to humans is unknown. We undertook this study to evaluate the importance of RasGRP-4 in the pathogenesis of human and rat arthritis.**

Methods. **Synovial tissue from patients with rheumatoid arthritis (RA) and osteoarthritis (OA) were evaluated immunohistochemically for the presence of RasGRP-4 protein. Fibroblast-like synoviocytes (FLS) were isolated from synovial samples, and expression of RasGRP-4 was evaluated by real-time quantitative reverse transcription–polymerase chain reaction analyses. The proliferation potency of FLS was evaluated by exposing the cells to a RasGRP-4–specific small interfering RNA (siRNA). Finally, the ability of RasGRP-4–specific siRNAs to hinder type II collagen–induced arthritis in rats was evaluated to confirm the importance of the signaling protein in the disease.**

Results. **Unexpectedly, RasGRP-4 protein was detected in the synovial hyperplastic lining, where proliferating FLS preferentially reside. FLS isolated from tissues obtained from a subpopulation of RA patients expressed much more RasGRP-4 than did FLS from examined OA patients. Moreover, the level of RasGRP-4 transcript was correlated with the FLS proliferation rate. The ability of cultured FLS to divide was diminished when they were treated with RasGRP-4–specific siRNAs. The intraarticular injection of RasGRP-4–specific siRNAs also dampened experimental arthritis in rats.**

Conclusion. **RasGRP-4 is aberrantly expressed in FLS and helps regulate their growth. This intracellular signaling protein is therefore a candidate target for dampening proliferative synovitis and joint destruction.**

Rheumatoid arthritis (RA) is a chronic autoimmune disease characterized by inflammation of the joints (1). Although disease-modifying antirheumatic drugs (DMARDs) including biologics are often used to treat patients with RA, remission according to the Simplified Disease Activity Index (2) occurs in <50% of treated patients (1,3,4). Also problematic are the high costs of existing therapeutics, as well as the increased susceptibility of treated patients to opportunistic infections.

Fibroblast-like synoviocytes (FLS) are key players in inflammation and destruction of the joints of RA patients (5). Since FLS increase their expression of matrix metalloproteinases (MMPs) when they encounter tumor necrosis factor α (TNFα) (6) and other proin-

Supported by the Japanese Ministry of Health, Labor, and Welfare, the Japanese Ministry of Education, Culture, Sports, Science, and Technology, and the NIH (grant AI-059746).

[1]Michihito Kono, MD, PhD, Shinsuke Yasuda, MD, PhD, Hideyuki Koide, BA, Takashi Kurita, MD, PhD, Yuka Shimizu, MD, Yusaku Kanetsuka, MD, Kenji Oku, MD, PhD, Toshiyuki Bohgaki, MD, PhD, Olga Amengual, MD, PhD, Tetsuya Horita, MD, PhD, Tomohiro Shimizu, MD, Tokifumi Majima, MD, PhD, Takao Koike, MD, PhD, Tatsuya Atsumi, MD, PhD: Hokkaido University Graduate School of Medicine, Sapporo, Japan; [2]Richard L. Stevens, PhD: Harvard Medical School, Boston, Massachusetts.

Address correspondence to Shinsuke Yasuda, MD, PhD, Division of Rheumatology, Endocrinology, and Nephrology, Hokkaido University Graduate School of Medicine, N15 W7, Kita-ku, Sapporo 060-8638, Japan. E-mail: syasuda@med.hokudai.ac.jp.

Submitted for publication May 14, 2014; accepted in revised form October 14, 2014.

flammatory factors, one of the ways anti-TNFα therapy is effective in RA is by diminishing the ability of FLS and other cell types in the arthritic joint to produce the zymogen forms of MMPs and aggrecanases that proteolytically destroy the cartilage extracellular matrix (7). Of all the cells implicated in RA pathogenesis, FLS are perhaps the least well understood. Indeed, there is no currently approved therapeutic for RA that targets this cell directly. Thus, a better understanding of the role(s) of FLS in the pathogenesis of RA is needed, especially the factors and mechanisms that control their growth.

Mast cells (MCs) also have been linked with inflammation and damage to the joints in RA patients (8–10). Experimental arthritis was markedly reduced in MC-deficient $Kit^{W}/Kit^{W\text{-}v}$ and $Kitl^{S}/Kitl^{Sl\text{-}d}$ mice (11,12) and in transgenic C57BL/6 (B6) mice lacking MC-restricted tryptase–heparin complexes (13,14). Inflammatory arthritis is dependent on proinflammatory cytokines. In this regard, TNFα, interleukin-1β (IL-1β), and IL-6 released from activated MCs, macrophages, and other cell types in the arthritic joint induce nearby FLS to proliferate and increase their expression of proMMPs and proaggrecanases which are activated by varied MC proteases.

Ras guanine nucleotide–releasing protein 4 (RasGRP-4) is a calcium-regulated guanine nucleotide exchange factor (GEF) and diacylglycerol/phorbol ester receptor (15). It was initially cloned from IL-3–developed mouse bone marrow–derived MCs (BMMCs), and every examined MC from mice, rats, and humans expressed this intracellular signaling protein (15–17). While peripheral blood monocytes (18) and neutrophils (19) also express RasGRP-4, fibroblasts normally do not (15,17,20).

Four members of the RasGRP family of signaling proteins exist in mice and humans, and dysregulation of RasGRP expression can have profound in vivo and in vitro consequences. For example, forced expression of RasGRP-1 (21,22), RasGRP-2 (23), RasGRP-3 (24), or RasGRP-4 (15,17,20) in normal fibroblasts led to decreased contact inhibition and increased proliferation when the transfectants were subsequently exposed to low levels of phorbol myristate acetate (PMA). These findings raised the possibility that the presence of a RasGRP in the wrong cell type can cause dysregulation of its growth rate, thereby increasing its susceptibility to transformation. In this regard, the insertion of mouse leukemia viruses into the 5′-flanking regions or introns of the RasGRP-1 gene or the RasGRP-2 gene or at a chromosome 7A3-B1 site near where the RasGRP-4 gene resides can lead to myeloid leukemia, B cell lymphomas, or T cell lymphomas in mice (25,26). In support of the pro-oncogenic activity of this family of GEFs, many of the human RasGRP-4 expressed sequence tags (ESTs) in the GenBank database originated from clear cell tumors of the kidney. Moreover, a RasGRP-4 complementary DNA was isolated from a patient with acute myelogenous leukemia (20).

Using a homologous recombination approach, Adachi and coworkers recently created a RasGRP-4–null B6 mouse line (27). The MCs in the tissues of these animals were morphologically normal but functionally defective in terms of their ability to exocytose many of the cell's mediators when activated. The finding that calcium ionophore– or PMA-treated BMMCs developed from RasGRP-4–null mice contained fewer TNFα and IL-1β transcripts than similarly treated wild-type mouse BMMCs raised the possibility that RasGRP-4 participates in signaling pathways that result in the generation and/or release of varied proinflammatory mediators from MCs and possibly other cell types in the synovium that are essential for joint inflammation and destruction. The RasGRP-4+ cells in mouse synovium that are essential in K/BxN arthritis induced by anti–glucose-6-phosphate isomerase autoantibodies have not yet been identified. Nevertheless, the finding that experimental arthritis could not be induced in RasGRP-4–null B6 mice documented for the first time an essential role for this GEF in the effector phase of the IgG/C5a-mediated murine arthritis model (27). In support of these mouse data, we identified defective isoforms of RasGRP-4 in the peripheral blood mononuclear cells of a subset of patients with RA (18).

Because MCs play prominent roles in one experimental arthritis model, we assumed that the inability to induce K/BxN arthritis in RasGRP-4–null mice was primarily a consequence of dysregulation of the proinflammatory MCs in the animal's synovium. Unexpectedly, we now show that most of the RasGRP-4+ cells in the human arthritic joint are cadherin 11–positive FLS rather than MCs and that the aberrant expression of this GEF in FLS contributes to their proliferation and thereby the development of arthritis. RasGRP-4 is therefore important in both MC- and FLS-dependent inflammatory arthritis.

PATIENTS AND METHODS

Preparation of synovial tissue and FLS. Synovial tissue specimens were acquired during synovectomy or joint replace-

Table 1. Characteristics of the RA and OA patients in this study*

	Histologic examination		Examination of cultured FLS	
	RA patients	OA patients	RA patients	OA patients
No. of women/men	7/2	5/0	8/2	10/0
Age at operation, years	70 (58–78)	73 (63–80)	66 (33–78)	72 (58–80)
Disease duration, years	11 (5–48)	NA	10.5 (2–48)	NA
Serum CRP, mg/dl	0.16 (0.02–5.69)	0.05 (0.02–0.32)	0.12 (0.02–5.69)	0.1 (0.02–0.61)
MMP-3, mg/dl	95.7 (44.8–449.9)	NA	90.5 (31.3–449.9)	NA
RF, units/ml	12 (1.1–82.8)	NA	16.4 (1.1–82.8)	NA
ACPAs, units/ml	115 (4.5–300)	NA	115 (4.5–300)	NA
Swollen joint count	3 (1–6)	NA	3 (1–6)	NA
Tender joint count	2 (0–16)	NA	3 (0–16)	NA
DAS28-ESR	4.4 (2.4–5.0)	NA	4.3 (2.4–5.0)	NA
HAQ DI score	1 (0–1.75)	NA	1 (0–1.75)	NA
Methotrexate use, no. (%)	5 (56)	0 (0)	5 (50)	0 (0)
Biologic agent use, no. (%)	4 (44)†	0 (0)	6 (60)‡	0 (0)

* Except where indicated otherwise, values are the median (range). RA = rheumatoid arthritis; OA = osteoarthritis; FLS = fibroblast-like synoviocytes; NA = not available; CRP = C-reactive protein; MMP-3 = matrix metalloproteinase 3; RF = rheumatoid factor; ACPAs = anti–citrullinated protein antibodies; DAS28-ESR = Disease Activity Score in 28 joints using the erythrocyte sedimentation rate; HAQ DI = Health Assessment Questionnaire disability index.
† Two patients (22%) were taking tocilizumab and 2 patients (22%) were taking infliximab.
‡ Two patients (20%) were taking tocilizumab, 2 patients (20%) were taking infliximab, 1 patient (10%) was taking etanercept, and 1 patient (10%) was taking golimumab.

ment surgery from 10 patients with RA and 10 patients with osteoarthritis (OA), after written informed consent. The patients' characteristics and clinical features are summarized in Table 1. This study was approved by the Human Ethics Committee of Hokkaido University Hospital, and every RA patient fulfilled the American College of Rheumatology/European League Against Rheumatism 2010 classification criteria for RA (28). Tissue was harvested and collected in phosphate buffered saline (PBS). A portion of the obtained synovial tissue in each instance was evaluated histochemically and immunohistochemically. Depending on the amount of tissue obtained, another portion in each tissue specimen was used for generating the FLS that were investigated in this study.

As previously reported (29), the synovium was removed, minced, and placed in 10 ml Hanks' balanced salt solution containing type I collagenase (Sigma). After a 2-hour digestion at 37°C, each digest was sequentially passed through a metal mesh and then a nylon mesh with 100-μm pores. The liberated cells were collected by centrifugation and placed in a 75-cm^2 culture flask containing 15 ml of Iscove's modified Dulbecco's medium (IMDM; Sigma) supplemented with 10% heat-inactivated fetal bovine serum (FBS), 100 IU/ml penicillin, and 100 μg/ml streptomycin (Sigma). The liberated cells were then cultured at 37°C in a humidified atmosphere of 5% CO_2. FLS at passages 3–6 were subjected to the experimental procedures noted below. Other investigators previously showed that their FLS expressed Hsp47/serpin H1 (30). As assessed immunohistochemically, >97% of the cells in our FLS cultures expressed this collagen chaperone protein and serine protease inhibitor. In contrast, none of the cells in the cultures expressed the monocyte/macrophage protein CD14. In addition, none of the cells became metachromatic when stained with toluidine blue, as do MCs (results not shown).

Immunohistochemistry of human synovial tissue. Synovial tissues from our arthritis patients were placed in Tissue Fixative (GenoStaff), embedded in paraffin, and sectioned at 6 μm. The resulting sections were deparaffinized, washed in ethanol, and rehydrated in PBS. Endogenous peroxidase activity was blocked with 0.3% H_2O_2 in PBS. The treated sections were rinsed, incubated for 10 minutes with G-Block (GenoStaff), and then incubated overnight in PBS containing anti-human RasGRP-4 antibody (Abcam), a polyclonal goat anti-human cadherin 11 antibody (R&D Systems), a monoclonal mouse anti-human CD14 antibody (Abcam), a mouse monoclonal anti-human CD68 antibody (Dako), or a mouse monoclonal anti-human Hsp47 antibody (Enzo Life Sciences). Normal rabbit IgG (Dako), goat IgG (Santa Cruz Biotechnology), mouse IgG2a (R&D Systems), mouse IgG (Santa Cruz Biotechnology), or mouse IgG2b (R&D Systems) served as the respective negative controls. After a wash, the secondary biotin-labeled anti-rabbit, anti-goat, or anti-mouse antibody (Dako) was added. Horseradish peroxidase–labeled streptavidin (Nichirei Biosciences) was used to detect the antigen. Some sections were stained with hematoxylin and eosin (H&E) or toluidine blue.

Synovial tissues from 9 RA patients and 5 OA patients were evaluated immunohistochemically for the presence of RasGRP-4 protein, and the RasGRP-4+ area in the cadherin 11–positive lining portion from the joint of each patient was quantified. Since the lining area increased in parallel to the amount of FLS hyperplasia, the RasGRP-4+ lining area was adjusted to the linear horizontal length (μm^2/μm) of the analyzed lining (30).

Real-time quantitative reverse transcription–polymerase chain reaction (qRT-PCR) analyses. Total RNA was obtained using TRIzol RNA Reagent (Life Technologies) according to the manufacturer's instructions. The RNA sam-

ples were reverse-transcribed using SuperScript VILO (Invitrogen). A standard qRT-PCR approach was then used to monitor the levels of the RasGRP-4 transcript in the FLS from 10 patients with RA and 10 patients with OA. In these experiments, the level of the RasGRP-4 transcript was normalized to that of the GAPDH transcript with an Applied Biosystems 7500 Real-Time PCR System and TaqMan MGB primers specific for the transcripts that encode RasGRP-4 (primer set Hs01073180_m1) and GAPDH (primer set Hs99999905_m1). Relative quantification was performed using the C_t method in which ΔC_t is the level of the RasGRP-4 transcript in the RNA sample relative to that of the GAPDH transcript. The difference in the expression of the RasGRP-4 transcripts among each sample was defined as fold changes in messenger RNA (mRNA) levels by $2^{-\Delta\Delta C_t}$.

Cell proliferation assay and effect of TNFα on the expression of RasGRP-4 in cultured human FLS. A qRT-PCR approach was used to evaluate the ability of TNFα to regulate the expression of RasGRP-4 in cultured FLS (n = 6). After washing with PBS, 7.5×10^5 FLS in 15 ml IMDM (supplemented with 100 IU/ml penicillin, 100 μg/ml streptomycin, and 10% heat-inactivated FBS) were added. Seventeen hours later, TNFα (Sigma) was added to the culture medium to achieve 10 or 100 ng/ml concentrations of the cytokine. After a 48-hour incubation at 37°C, the untreated and TNFα-treated FLS were lysed following the addition of 750 μl TRIzol.

In replicate cultures, the proliferation of TNFα-treated FLS also was evaluated using the tetrazolium/formazan assay. After washing with PBS, 3×10^3 FLS in 100 μl IMDM containing 10% heat-inactivated FBS, penicillin, and streptomycin were added to each well of a CellTiter 96 Proliferation Assay Kit (Promega). Different concentrations (0, 10, or 100 ng/ml) of human TNFα (Sigma) were added to the medium. Following a 5-day incubation at 37°C, 100 μl of the dye solution in the assay kit was added to each well and the treated cells were incubated for another 4 hours at 37°C. Each reaction was terminated using the kit's stop solution, and the resulting optical density at 570 nm was measured. These proliferation assays were done in triplicate, and the experiments were carried out before the FLS became confluent in the culture dishes.

Small interfering RNA (siRNA) knockdown of RasGRP-4 levels in cultured human FLS. An siRNA approach was used to diminish the levels of RasGRP-4 transcript (and thereby the levels of protein) in FLS from our RA patients (n = 4). After washing FLS with PBS, 7.5×10^5 cells in 15 ml IMDM containing 10% heat-inactivated FBS were added. The next day, the medium was changed to Opti-MEM I medium (Life Technologies), and the cells were transfected with a solution containing 10 n*M* siRNA (Applied Biosystems) with 3 n*M* Lipofectamine RNAiMAX (Life Technologies). For these experiments, the company's Silencer Select Negative Control No. 1 siRNA was used, as were the Silencer Select Pre-Designed siRNAs s41861 and s41862 that targeted exons 12 and 10, respectively, in the normal, full-length isoform of human RasGRP-4 (15). After a 6-hour incubation at 37°C, the medium was changed to siRNA-free IMDM containing 10% heat-inactivated FBS. After a 48-hour incubation at 37°C, the treated FLS were collected and total RNA was isolated. The levels of the transcripts that encode RasGRP-4, RANKL (primer set Hs00243522_m1), IL-6 (primer set Hs00985639_m1), vascular endothelial growth factor (VEGF; primer set Hs00900055_m1), MMP-1 (primer set Hs00899658 m1), MMP-3 (primer set Hs00968305_m1), and microsomal prostaglandin E synthase 1 (mPGES-1; primer set Hs01115610_m1) in the treated human FLS were quantified and normalized against that of the housekeeping transcript that encodes GAPDH. TaqMan primers specific for each transcript were used.

Cell proliferation assays also were performed on replicate siRNA-treated FLS from our RA patients (n = 4). After washing with PBS, 1×10^5 FLS in 100 μl Opti-MEM I medium were added to each well of a CellTiter 96 Proliferation Assay Kit. After a 48-hour incubation at 37°C, the tetrazolium/formazan proliferation assay was performed.

Importance of RasGRP-4 in collagen-induced arthritis (CIA) in rats. Using the disease model developed by Earp and coworkers (31), CIA was induced in fifteen 7-week-old female Lewis rats by immunizing each animal at the base of the tail with 200 μl of a 1 mg/ml solution of porcine type II collagen (Chondrex) dissolved in 0.05*M* acetic acid and emulsified 1:1 in Freund's incomplete adjuvant (Chondrex). Seven days later, the animals received a booster injection of the collagen antigen emulsified in Freund's incomplete adjuvant. The experimental protocol was approved by the Animal Ethics Committee at Hokkaido University. On day 14, 5 rats in each experimental group received an intraarticular injection, into both the right and left ankle joints, of a 50-μl solution that contained a 10-μ*M* siRNA–atelocollagen (Koken) complex. The 5 rats in the first group received the negative control siRNA–atelocollagen complex. We used atelocollagen because siRNA–atelocollagen complexes are resistant to nucleases and are efficiently transduced into cells, thereby allowing long-term gene silencing (32). The 5 rats in the second group received the first siRNA, s139320, which targeted the sixth exon of the rat RasGRP-4 gene. Finally, the 5 rats in the third group received the second siRNA, s139321, which targeted the twelfth exon of the rat RasGRP-4 gene.

On days 0, 7, 14, 17, 21, 24, 28, 31, and 35, the control and RasGRP-4–specific siRNA–treated arthritic animals were examined for visual signs of disease, defined as macroscopic evidence of increased paw thickness and ankle diameter. Arthritis was scored from 0 (no erythema and swelling) to 4 (erythema and severe swelling that encompassed the ankle, foot, and digits or ankylosis of the limb) (33). The accuracy of the scoring system was verified by micro–computed tomography (micro-CT) (R_mCT2; Rigaku) coupled with histologic analysis of representative arthritic limbs. Radiographic severity in rats with CIA was assessed in a blinded manner on day 35. Micro-CT of the ankles was performed on all animals. The treated rats were given a score of 0 (normal joint) to 3 (severe cartilage and bone erosions) for each ankle, based on the extent of soft tissue swelling, joint space narrowing, bone destruction, and periosteal new bone formation (34).

Rats were killed on day 35 for histopathologic and immunohistochemical analyses. The ankles were decalcified and embedded in paraffin, and serial sections were stained with anti–RasGRP-4 antibody, H&E, or toluidine blue for

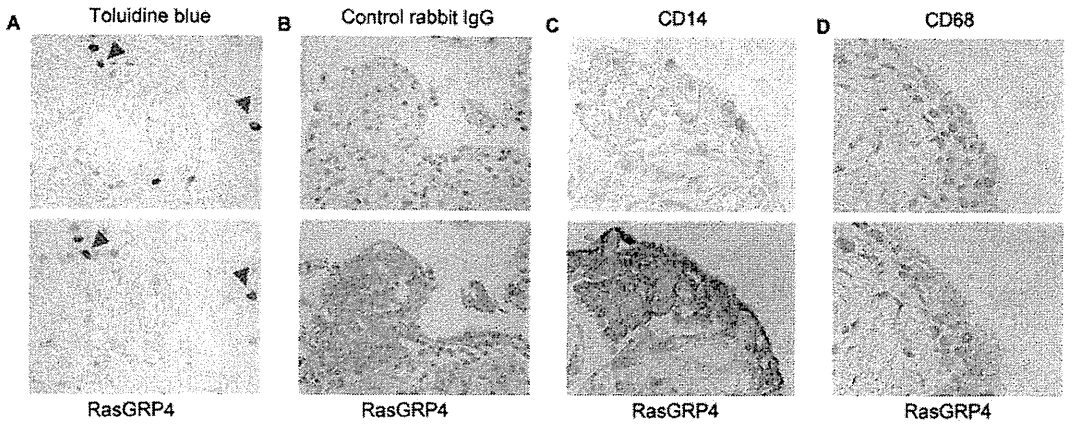

Figure 1. Ras guanine nucleotide–releasing protein 4 (RasGRP-4) protein is abundant in synovial mast cells (MCs) but not in synovial macrophages. **A,** Serial sections of synovium from patients with rheumatoid arthritis were stained with toluidine blue or anti–RasGRP-4 antibody. **Arrowheads** indicate toluidine blue–positive MCs or RasGRP-4+ MCs in synovium from these patients. **B–D,** Serial sections were stained with anti–RasGRP-4 antibody (**B–D**) or with control rabbit IgG (**B**), anti-CD14 antibody (**C**), or anti-CD68 antibody (**D**). While RasGRP-4 protein was abundant in synovial MCs and in an undefined cell type, this guanine nucleotide exchange factor was not abundant in CD14+CD68+ macrophages. Original magnification × 400 in **A** and **B**; × 600 in **C** and **D**.

microscopic examination. Inflammation was scored on a scale of 0 (no inflammation) to 3 (severely inflamed joint) depending on the number of inflammatory cells in the synovial cavity (exudate) and synovial tissue (infiltrate). Exudate and inflammatory infiltrate were scored individually. Cartilage destruction was scored on a scale of 0 to 3, where 0 corresponds to no cartilage loss and 3 corresponds to complete loss of articular cartilage. Loss of bone was scored on a scale of 0 (no damage) to 5 (loss of cartilage and bone) (35). Anti-human RasGRP-4 antibody was also used to evaluate the effects of siRNAs used in this rat CIA model. The RasGRP-4+ lining area was adjusted to the linear horizontal length ($\mu m^2/\mu m$) of the analyzed lining as done in human synovial tissues.

Statistical analysis. For cross-sectional analyses, quantitative variables were compared by Welch's *t*-test. Changes in quantitative variables after siRNA treatment were tested by the Kruskal-Wallis test with a post hoc test. Correlation between different numerical variables was analyzed by Pearson's test. *P* values less than 0.05 were considered significant.

RESULTS

Immunohistochemistry findings in human synovial tissue. As assessed immunohistochemically with anti–RasGRP-4 antibody, toluidine blue–positive MCs in arthritic human synovium contained RasGRP-4 protein (Figure 1A), as anticipated. While RasGRP-4 was not abundant in CD14+CD68+ mature macrophages (Figures 1C and D), as also anticipated, the GEF was prominently expressed in hyperplastic lining areas of RA synovium (Figures 1B–D and 2), with lower levels in OA synovium (Figure 2). Others have reported that FLS express cadherin 11 (36) and Hsp47 (30). Unexpectedly, most RasGRP-4+ cells in synovium from our RA patients were cadherin 11–positive Hsp47+ FLS rather than MCs. Moreover, RasGRP-4+ areas were significantly increased in synovial tissues from our RA patients compared with those from our OA patients (Figure 2D).

Quantitation of RasGRP-4 transcript levels in FLS derived from RA and OA patients. Using a qRT-PCR approach, levels of RasGRP-4 transcripts were quantified in early passages of cultured FLS from patients with RA or OA. FLS from some RA patients contained substantial amounts of RasGRP-4 mRNA (Figure 3A), thereby supporting immunohistochemical findings in synovial tissues from these patients. Nucleotide sequence analysis of the primary qRT-PCR product from RA patient 3 confirmed that the evaluated transcript in the mRNA assay encoded full-length RasGRP-4 rather than its homologous family members RasGRP-1, RasGRP-2, or RasGRP-3. FLS from 5 of 6 RA patients who had been treated with biologic agents contained lower amounts of RasGRP-4 mRNA. In this regard, RA patients 3 and 4 had been given the anti–IL-6 receptor tocilizumab, whereas RA patients 5–8 had been given anti-TNFα agents (infliximab in patients 5 and 7, golimumab in patient 6, and etanercept in patient 8). Levels of RasGRP-4 transcript were correlated with the rate of proliferation of FLS ($R^2 = 0.67$, $P < 0.01$) (Figure 3B).

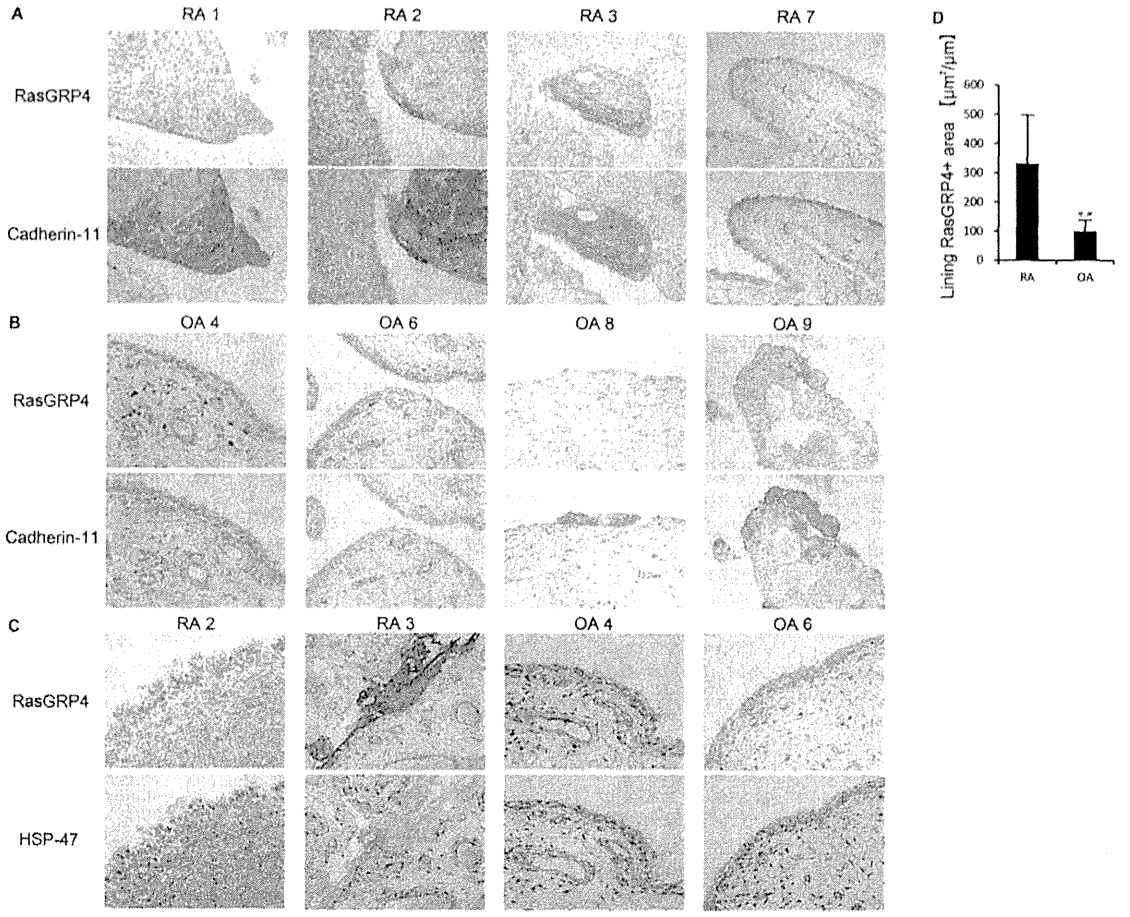

Figure 2. Fibroblast-like synoviocytes (FLS) in the hyperplastic lining area of the synovium of a subset of rheumatoid arthritis (RA) patients contain appreciable amounts of Ras guanine nucleotide–releasing protein 4 (RasGRP-4) protein. **A–C,** Serial sections from different RA and osteoarthritis (OA) patients were stained with anti–RasGRP-4 antibody (**A–C**), anti–cadherin 11 antibody (**A** and **B**), or anti-Hsp47 antibody (**C**). Cadherin 11–positive Hsp47+ FLS in hyperplastic lining areas of synovium from a number of RA patients often contained immunoreactive RasGRP-4 protein. **D,** The cadherin 11–positive lining area of synovium from the RA patients (n = 9) contained more RasGRP-4 protein than did the corresponding area of synovium from the OA patients (n = 5). Values are the mean ± SD. ** = $P < 0.01$ versus RA patients, by Welch's *t*-test. Original magnification × 400.

TNFα induces RasGRP-4 expression in FLS, and steady-state proliferation of FLS depends in part on RasGRP-4. As previously reported (5,37,38), TNFα-treated FLS proliferated significantly faster than FLS that did not encounter this proinflammatory cytokine (Figure 3D). Because the levels of RasGRP-4 transcript were significantly higher in TNFα-treated FLS (Figure 3C), an siRNA approach was used to determine whether these observations were directly linked. Levels of RasGRP-4 transcript in FLS treated with 1 of 2 different siRNAs specific for human RasGRP-4 were significantly decreased compared with levels of RasGRP-4 transcript in untreated FLS (mock) or cells treated with control siRNA (Figure 4A). FLS isolated from our RA patients also decreased their proliferation activity when exposed to the RasGRP-4–specific siRNAs (Figure 4B).

FLS-derived RANKL, IL-6, VEGF-A, MMP-1, MMP-3, and mPGES-1 work in synergy to promote the development of RA (39). Decreased RasGRP-4 expression in RasGRP-4–specific siRNA–treated FLS did not lead to decreased levels of transcripts that encode RANKL, IL-6, VEGF-A, and MMP-3 (Figure 4C),

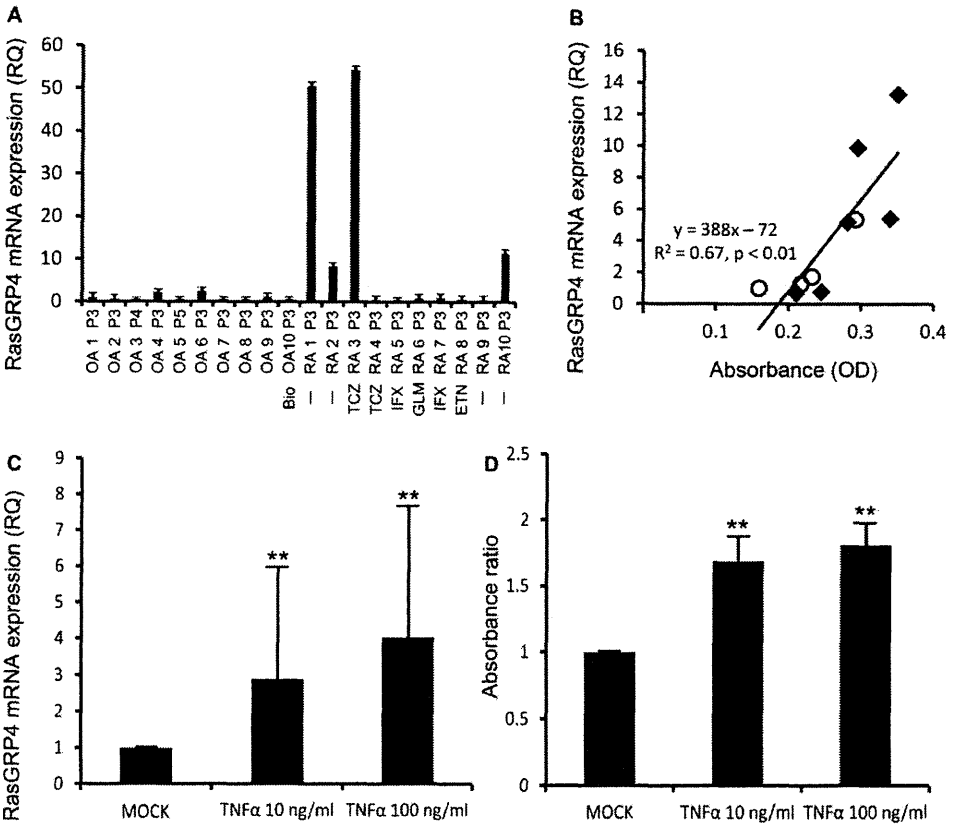

Figure 3. Evaluation of RasGRP-4 mRNA levels in FLS and proliferation of these cells. **A,** High levels of RasGRP-4 transcript in FLS from RA patients 1, 2, 3, and 10. RA patients 3 and 4 had been given tocilizumab (TCZ), RA patients 5 and 7 had been given infliximab (IFX), RA patient 6 had been given golimumab (GLM), and RA patient 8 had been given etanercept (ETN). **B,** Correlation of the presence of RasGRP-4 transcript with rate of proliferation of these FLS. Diamonds and circles correspond to FLS from RA patients (n = 6) and OA patients (n = 4), respectively. **C,** Evaluation of RasGRP-4 mRNA levels in FLS (n = 6) following mock stimulation or stimulation with the indicated concentrations of tumor necrosis factor α (TNFα). **D,** Proliferation of FLS (n = 6) following mock stimulation or stimulation with the indicated concentrations of TNFα. Values are the mean ± SEM (**A**) or the mean ± SD (**C** and **D**). ** = $P < 0.01$ versus mock, by Welch's t-test. RQ = relative quantification; P = passage; Bio = biologic agents (see Figure 2 for other definitions).

suggesting that RasGRP-4 is not essential for the expression of those 4 proteins at the mRNA level in the arthritic joint. In contrast, levels of MMP-1 and mPGES-1 transcripts were significantly decreased in FLS treated with a RasGRP-4 siRNA (Figure 4C), implying that these 2 proteins were under the control of this signaling protein.

Assessment of CIA in rats. Compared with type II collagen–immunized animals injected with control siRNA, intraarticular injection of siRNAs specific for rat RasGRP-4 significantly improved both the clinical arthritis score and the ankle diameter in arthritic rats immunized with type II collagen (Figure 5A). Micro-CT revealed that arthritic rats injected with a RasGRP-4–specific siRNA had significantly lower erosion scores compared to animals injected with control siRNA (Figure 5B). Anti-human RasGRP-4 antibody recognized rat MCs as well as proliferative lining area in arthritic synovial tissue, but control IgG did not (results not shown). Thus, this antibody cross-reacted with rat RasGRP-4 by immunohistochemistry, although the signal intensities were somewhat weaker compared with those seen in human tissues. The RasGRP-4+ area in the synovial lining was significantly decreased in relevant tissues of rats that received intraarticular injections of RasGRP-4–specific siRNA–atelocollagen complexes,

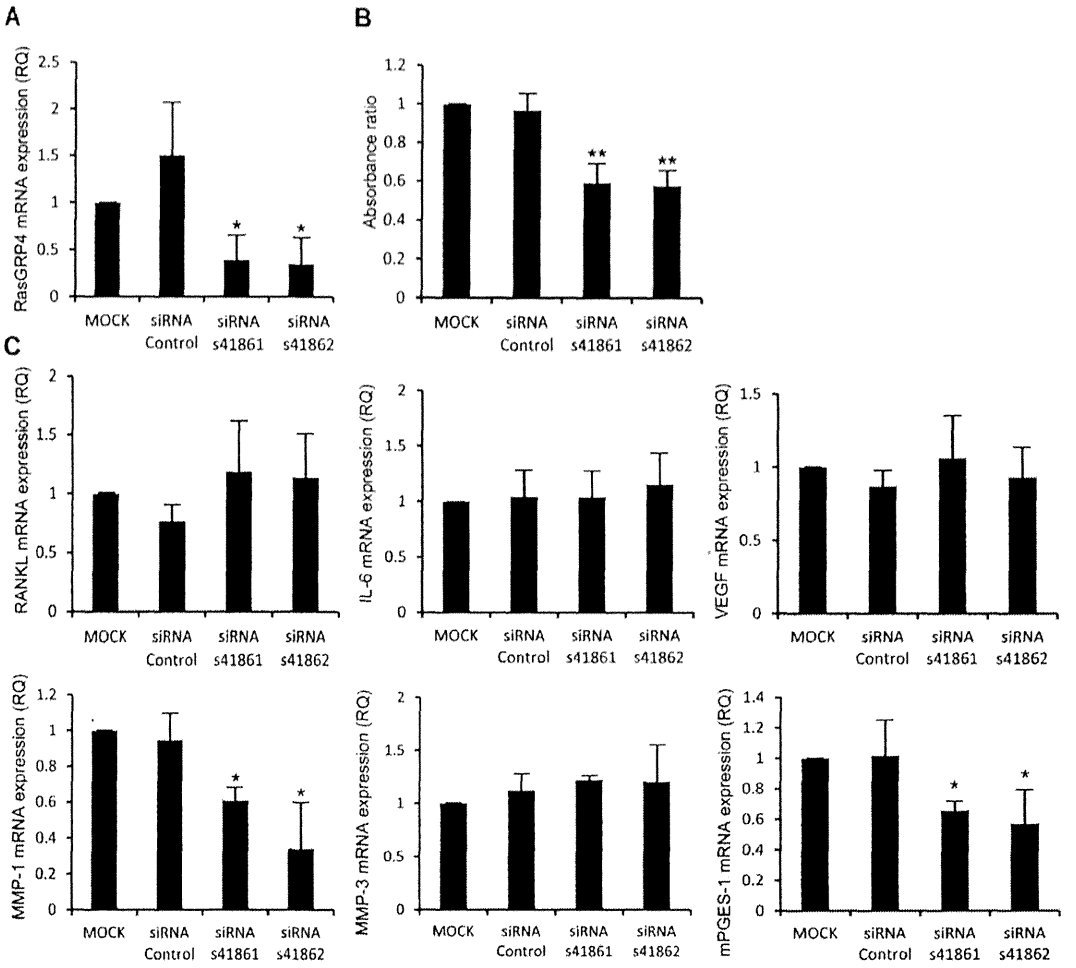

Figure 4. Effect of knockdown of RasGRP-4 levels in FLS from RA patients (n = 4). **A** and **B**, The effects of small interfering RNAs (siRNAs) on RasGRP-4 mRNA levels in FLS from RA patients (**A**) and on proliferation rates of these FLS (**B**) were evaluated following mock treatment or treatment with control siRNA or siRNA s41861 or s41862. **C**, Levels of transcripts that encode RANKL, interleukin-6 (IL-6), vascular endothelial growth factor (VEGF), matrix metalloproteinase 1 (MMP-1), MMP-3, and microsomal prostaglandin E synthase 1 (mPGES-1) were measured in FLS that were treated with a control siRNA or 1 of 2 siRNA specific for human RasGRP-4. Values are the mean ± SD. * = $P < 0.05$; ** = $P < 0.01$ versus mock and siRNA control, by Welch's *t*-test. RQ = relative quantification (see Figure 2 for other definitions).

compared with rats that received intraarticular injections of control siRNA (Figure 5C). Arthritic rats that received RasGRP-4–specific siRNAs had significantly lower exudate scores, inflammatory infiltrate scores, cartilage destruction scores, and bone erosion scores in ankle joints relative to arthritic animals that received control siRNA (Figure 5D). On the other hand, there was no histologic difference in the knee joints (data not shown).

DISCUSSION

The FLS is the major cell type in the synovium that invades the joints of patients with RA. This mesenchymal cell plays significant adverse roles in the initiation and perpetuation of destructive joint inflammation. Cadherin 11 is an adhesion protein that participates in the homotypic aggregation of FLS (36). Izquierdo and coworkers (30) reported that the collagen-specific mo-

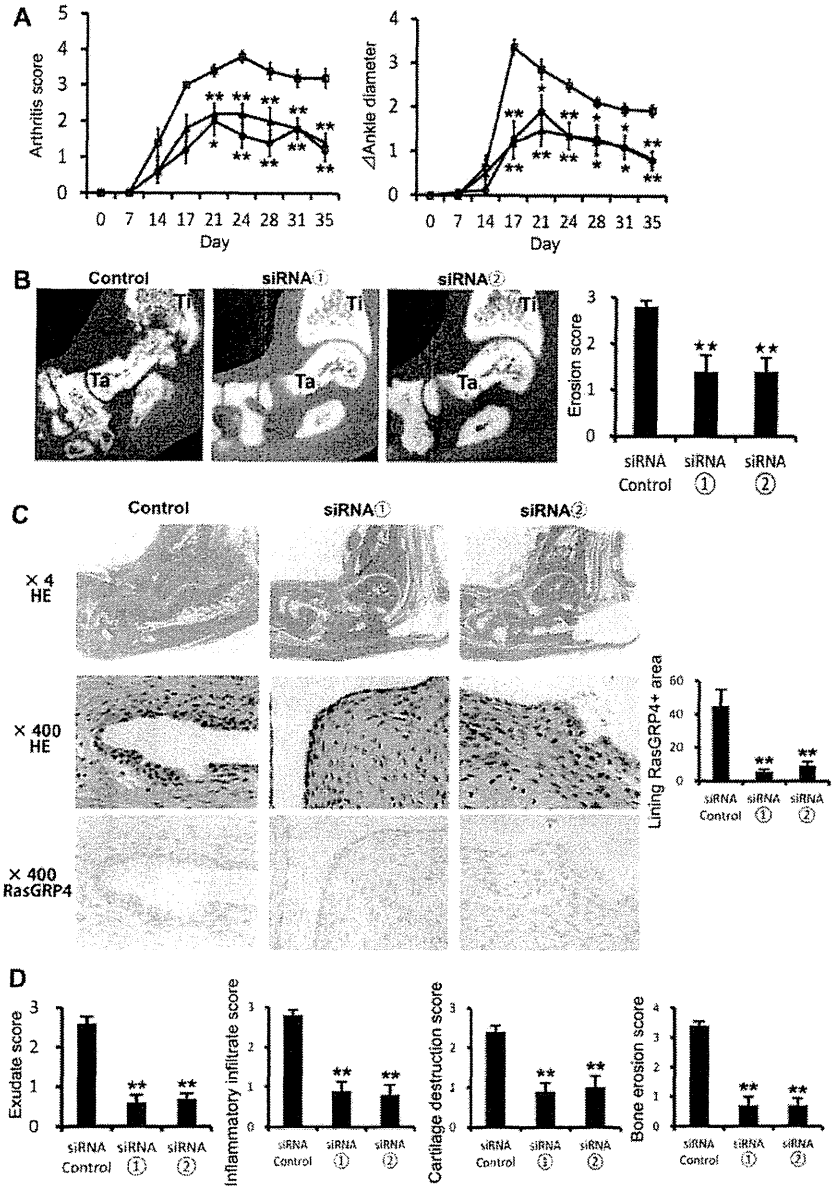

Figure 5. Intraarticular injection of a Ras guanine nucleotide–releasing protein 4 (RasGRP-4)–specific small interfering RNA (siRNA) hinders the development of collagen-induced arthritis (CIA) in rats. **A,** CIA was induced in rats, and arthritis scores and ankle diameters were monitored for 35 days. One group of animals (n = 10 legs) received control siRNA (squares). The second group (n = 10 legs) and third group (n = 10 legs) received the RasGRP-4–specific siRNAs s139320 (siRNA 1; triangles) and s139321 (siRNA 2; circles), respectively. **B,** Representative micro–computed tomography images show arthritic rats given control siRNA, siRNA 1, or siRNA 2. **Ti** = tibia; **Ta** = talus. Erosion scores in each group of animals were determined (n = 10 legs per group). **C,** Representative images show hematoxylin and eosin (H&E) staining and immunohistochemistry using anti-human RasGRP-4 antibodies in arthritic rats given control siRNA, siRNA 1, or siRNA 2. The RasGRP-4+ area in the synovial lining was compared among these 3 groups. **D,** Shown are exudate scores, inflammatory infiltrate scores, cartilage destruction scores, and bone erosion scores in arthritic rats treated with control siRNA or RasGRP-4 siRNAs. Values are the mean ± SEM. * = $P < 0.05$; ** = $P < 0.01$ versus control siRNA.